https://doi.org/10.5194/amt-2021-46
Preprint. Discussion started: 29 March 2021


Atmospheric Measurement Techniques Discussions

# Determination of the multiple-scattering correction factor and its cross-sensitivity to scattering and wavelength dependence for different AE33 Aethalometer filter tapes: A multi-instrumental approach

Jesús Yus-Díez[1,2], Vera Bernardoni[3], Griša Močnik[4,5], Andrés Alastuey[1], Davide Ciniglia[3], Matic Ivančič[6], Xavier Querol[1], Noemí Perez[1], Cristina Reche[1], Martin Rigler[6], Roberta Vecchi[3], Sara Valentini[3], and Marco Pandolfi[1]

[1]Institute of Environmental Assessment and Water Research (IDAEA-CSIC), C/Jordi Girona 18-26, 08034, Barcelona, Spain
[2]Grup de Meteorologia, Departament de Física Aplicada, Universitat de Barcelona, C/Martí i Franquès, 1, 08028, Barcelona, Spain
[3]Dipartimento di Fisica "A. Pontremoli", Università degli Studi di Milano & INFN-Milan, via Celoria 16, 20133 Milano, Italy
[4]Center for Atmospheric Research, University of Nova Gorica, Vipavska 11c, SI-5270 Ajdovščina, Slovenia.
[5]Department of Condensed Matter Physics, Jozef Stefan Institute, Jamova 39, SI-1000 Ljubljana, Slovenia
[6]Aerosol d.o.o., Ljubljana, Slovenia

**Correspondence:** jesus.yus@idaea.csic.es

**Abstract.**

Accurate measurements of light absorption by aerosolized particles, especially black carbon (BC), are of utter importance since BC represents the second most important climate-warming agent after carbon dioxide ($CO_2$). Reducing the uncertainties related to the absorption measurement techniques will improve the global estimation of BC concentration and the radiative effects of light absorbing aerosols. Currently, one of the most widely used instruments for BC and absorption measurements is the dual-spot aethalometer, AE33, which derives the absorption coefficients of aerosol particles at 7 different wavelengths from the measurements of optical attenuation through a filter where particles are continuously collected. An accurate determination of the absorption coefficient relies on the quantification of non-linear processes related to the collection of sample on the filter. The multiple-scattering correction factor ($C(\lambda)$), which depends on the filter tape used and on the optical properties of the collected particles, is the parameter with the greatest uncertainty.

An in-depth analysis of the AE33 multiple-scattering correction factor and its wavelength dependence for different filter tapes, i.e. the old most referenced known as TFE-coated glass and the current most widely used M8060, has been carried out by comparing the AE33 attenuation measurements with the absorption measurements from different filter-based techniques. Online co-located multi-angle absorption photometer (MAAP) measurements and offline PP_UniMI polar photometer measurements were used with this aim. We used data from three different measurement stations in North-East of Spain: an urban background station (Barcelona; BCN), a regional background station (Montseny; MSY) and a mountain-top station (Montsec d'Ares; MSA). The median C values (at 637 nm) measured at the three stations ranged between 2.29 (at BCN and MSY; lowest 5th percentile of 1.97 and highest 95th percentile of 2.68) and 2.51 (at MSA; lowest 5th percentile of 2.06 and highest 95th

https://doi.org/10.5194/amt-2021-46
Preprint. Discussion started: 29 March 2021


Atmospheric Measurement Techniques Discussions

percentile of 3.06). The C factor was wavelength-dependent only at the mountain-top station, whereas at the urban and regional stations no statistically significant difference was found at the 7 different AE33 wavelengths. The wavelength-dependence of C at the mountain station was in part driven by the predominant effect of dust particles during Saharan dust outbreaks at this station. At the mountain station, neglecting the wavelength dependence of the C factor led to an underestimation of the Absorption Ångström Exponent (AAE) of 12%. The analysis of the cross-sensitivity to scattering for different filter tapes revealed a large increase of the C factor at the three stations when the single scattering albedo (SSA) of the collected particles was above 0.90-0.95, with up to a 3-fold increase above the average values. The result of the cross-sensitivity to scattering displayed a fitted constant multiple scattering parameter, $C_f$, of 2.21 and 1.96 and a cross-sensitivity factor, $m_s$, of 0.8% and 1.7% for MSY and MSA stations, respectively, for the TFE-coated glass filter tape. For the M8060 filter tape, $C_f$ of 2.50, 1.96, 1.82 and a $m_s$ of 0.7%,1.5%, 2.7%, for BCN, MSY and MSA stations, respectively, were obtained. Differences in the absorption coefficient determined from AE33 measurements at BCN, MSY and MSA of around a 35-40 % can be expected when using the site-dependent C determined experimentally instead of the nominal C value.

## 1 Introduction

Atmospheric aerosol particles play an important role on the Earth's radiative balance directly by scattering and absorbing solar and terrestrial radiation and indirectly by acting as cloud condensation nuclei. Large uncertainties still exist on the effects that atmospheric particles have on climate (Myhre et al., 2013). In fact, the aerosol-radiation interaction depends on aerosol properties such as aerosol size distribution, mixing state, and refractive index, among others (e.g. Bond et al., 2013). Furthermore, no standard reference material currently exists for instrument calibration to determine the aerosol particles optical properties. Globally, aerosols have helped to reduce the warming effect from greenhouse gases because of their net cooling effect on climate (Myhre et al., 2013). However, this influence is likely to be reduced over the coming decades as air pollution measures are implemented around the world (Samset et al., 2018). Therefore, in order to properly constrain global models, it is necessary to better characterize the atmospheric absorption by aerosols from observations. Among the atmospheric aerosols, black carbon (BC), stands out as phenomenologically different, being the most efficient light absorbing aerosol component and being responsible for the second most important contribution to positive climate forcing after carbon dioxide (Myhre et al., 2013). However, there are still large uncertainties related to the radiative forcing of BC particles. In fact, the climate forcing potential of BC is influenced by BC properties which are strongly source and site dependent (Houghton, 2001; Kirchstetter et al., 2004a; Ramanathan and Carmichael, 2008; Myhre et al., 2013; Bond et al., 2013; Liu et al., 2015; Ramanathan et al., 2020). In addition to BC, atmospheric absorption by aerosol particles is also driven by specific organic compounds (e.g. from incomplete combustion, biomass smoldering, and secondary and biogenic sources) often referred to as Brown Carbon (BrC) and by mineral dust (e.g. Alfaro et al., 2004). Unlike BC, which absorbs radiation in a wide range of wavelengths (from UV to infrared) with a wavelength independent refractive index, BrC and mineral dust refractive index increases at shorter wavelengths, close to the UV range (Kirchstetter et al., 2004b; Andreae and Gelencsér, 2006; Bergstrom et al., 2007; Laskin et al.,

https://doi.org/10.5194/amt-2021-46
Preprint. Discussion started: 29 March 2021


Atmospheric Measurement Techniques Discussions

2015; Cappa et al., 2019). Therefore, having at disposal accurate absorption measurement techniques is crucial to determine particles light absorption which can afterwards be used in climate projections (Mengis and Matthews, 2020; Wang et al., 2020).

There are three main approaches in the literature to determine aerosol particles light absorption: by measuring the suspended particles in a cell, e.g. with photo-thermal interferometry or photo-acoustic techniques, and by either on-line or off-line filter-based photometer methods (e.g., Lin et al., 1973; Terhune and Anderson, 1977; Hansen et al., 1984; Stephens et al., 2003; Moosmüller et al., 2009; Ajtai et al., 2010; Vecchi et al., 2014). Among the indirect methods for measuring absorption, the "subtraction method", which does not rely on a filter, calculates the absorption from the difference between extinction and scattering by suspended particles (Singh et al., 2014). However, this method can lead to large errors at large single scattering albedo (SSA) values when the extinction is dominated by scattering (Onasch et al., 2015). On-line measurement methodologies based on particle suspension, such as the photo-acoustic spectroscopy (PAS) (Ajtai et al., 2010), have the advantage of measuring directly the absorption by particles suspended in a sampling cell avoiding filter-based artifacts. However, in the case of photo-acoustic spectroscopy measurements, the heating of the sample and the evaporation of coating materials on the sample may lead to higher detection limit and artifacts impairing the measurement accuracy (Lack et al., 2006; Linke et al., 2016). The photo-thermal interferometry (PTI) is an absorption measurement technique originally developed for measurements of trace gases that has also been applied to aerosol measurements (Lee and Moosmüller, 2020; Visser et al., 2020). However, the aforementioned techniques have so far proved difficult to deploy in a field setting thus limiting their broader use in international measurements networks. Filter-based instruments (either on-line or off-line) rely on the sampling of aerosol particles collected in a filter matrix and on the measurement, with a photometer, of the resulting change of light intensity, either on the transmittance (Hansen et al., 1984; Bond et al., 1999; Drinovec et al., 2015), or on both transmittance and reflectance (Petzold and Schönlinner, 2004). This method is affected by artifacts resulting mainly from the effects that the filter has on the measurements. Off-line in-house made filter based polar photometers, which measure both transmittance and reflectance, are deployed at some research centers. Examples are the MWAA (multi-wavelength absorption analyzer) deployed at University of Genoa (Massabò et al., 2013) and the PP_UniMI polar photometer deployed at University of Milan (Vecchi et al., 2014; Bernardoni et al., 2017). These methods can perform accurate absorption measurements by increasing the number of measuring angles (Massabò et al., 2013; Vecchi et al., 2014; Bernardoni et al., 2017) thus allowing an accurate determination of the filter artifacts.

The main advantage of the on-line filter-based methods is that these techniques are ease of use, allow for unattended operation, are relatively inexpensive and provide real-time data. For these reasons, these methods are widely used in international networks such as the Global Atmosphere Watch (GAW, World Meteorological Organization) and the European Research Infrastructure for the Observation of Aerosol, Clouds and Trace Gases (ACTRIS; www.actris.eu). The most used filter-based instruments are the Aethalometer (Hansen et al., 1984; Drinovec et al., 2015), the Particle Soot Absorption Photometer (PSAP, Bond et al., 1999), the Continuous Light Absorption Photometer (CLAP; Ogren et al., 2017), and the Multi-Angle Absorption Photometer (MAAP, Model 5012, Thermo, Inc., USA; Petzold and Schönlinner, 2004). The measured mass concentration of light absorbing carbonaceous aerosol inferred via optical attenuation of light is referred to as equivalent BC (eBC; Petzold et al., 2013). The main artifacts affecting the light absorption measurements of these instruments are the multiple light scat-

https://doi.org/10.5194/amt-2021-46
Preprint. Discussion started: 29 March 2021


Atmospheric Measurement Techniques Discussions

tering within the filter, the filter loading effect and the particle scattering correction (Liousse et al., 1993; Bond et al., 1999; Weingartner et al., 2003; Schmid et al., 2006; Collaud Coen et al., 2010; Lack et al., 2014). Algorithms for correcting these artifacts have been applied and their efficacy tested over the years (Weingartner et al., 2003; Arnott et al., 2005; Schmid et al., 2006; Virkkula et al., 2007; Collaud Coen et al., 2010; Virkkula et al., 2015).

The filter loading effect consists in the accumulation of particles and the consequent loss of sensitivity of the instrument with an increasing particle load (Bond et al., 1999; Weingartner et al., 2003; Lack et al., 2008; Moosmüller et al., 2009). The cross-sensitivity to scattering is the consequence of the multiple light scattering within the filter fibers and between particles and fibers, thus it is largely dependent on the single scattering albedo of the deposited aerosols. For the older Aethalometer model (AE31) the filter loading effect has been thoroughly studied and different methods for its quantification have been suggested. These methods use for example the discontinuity between the eBC concentration measurements before and after a filter spot is changed (Weingartner et al., 2003; Virkkula et al., 2007) or use the relationship between the eBC concentration and light attenuation (Park et al., 2010; Segura et al., 2014; Drinovec et al., 2015) to correct for filter loading effect. For the AE33 model the loading effect is corrected on-line using the dual-spot technology (Drinovec et al., 2015). In addition, the different physical and chemical properties of the collected particles influence particle optical properties such as the backscatter fraction and the single scattering albedo (SSA), thus affecting also the multiple scattering of the collected particles and the filter loading effect (Weingartner et al., 2003; Lack et al., 2008; Virkkula et al., 2015; Drinovec et al., 2017). Among the on-line filter-based instruments, the Multi Angle Absorption Photometer (MAAP) uses also the measurements of light scattered by the blank and loaded filter to take into account for both the loading effect and the aerosol particles multiple scattering. Consequently, the MAAP directly provides particle absorption coefficients similar to those obtained with other types of instruments (e.g. PAS; Petzold and Schönlinner, 2004; Petzold et al., 2005).

Currently, due to the described limitations of the filter-based photometers and other in-situ methods, no reference technique for measuring aerosol particles light absorption is available (Petzold et al., 2013; Lack et al., 2014). In the multi-wavelength dual-spot Aethalometer (AE33, Magee Scientific, Aerosol d.o.o. - Drinovec et al., 2015) the loading effect is corrected on-line and, furthermore, the AE33 software directly implements the use of a correction factor (C) related to the multiple scattering within the filter matrix to convert the measured attenuation to an absorption coefficient. This C factor is generally assumed a-priori, but it can be experimentally determined by using independent absorption measurements or by comparisons with other filter photometers(e.g. Weingartner et al., 2003; Arnott et al., 2005; Drinovec et al., 2015; Backman et al., 2017). For previous filter tapes and aethalometer versions different values of the multiple scattering parameter have been reported: for the AE31 quartz filter Weingartner et al. (2003) proposed a value of 2.14 which later on was recommended to be 3.5, i.e. larger by a factor of 1.64 (Müller, 2015; WMO, 2016); for the AE33 Drinovec et al. (2015) found a C of 1.57 for the Pallfex Teflon-coated glass fiber (TFE-coated glass), which, after re-normalization using the factor 1.64, resulted in C=2.57. Moreover, different experimental C factor values have been obtained ranging between 2.57-4.24 (Müller et al., 2011b; Drinovec et al., 2020; Laing et al., 2020; Valentini et al., 2020a; Bernardoni et al., 2020). In addition, these filters have been found to feature a cross-sensitivity to scattering, $\mathrm{m_s}$, ranging between 1 and 5% (Müller, 2015; Drinovec et al., 2015; Zhang et al., 2018; Corbin et al., 2018; Laing et al., 2020; Drinovec et al., 2020). To the best of our knowledge, so far no in-situ ambient measurements have

https://doi.org/10.5194/amt-2021-46
Preprint. Discussion started: 29 March 2021


Atmospheric Measurement Techniques Discussions

been reported in literature for the recommended new M8060 filter tape and no sensitivity studies of the cross-sensitivity to scattering of the C factor have been carried out for this new filter tape either.

The recent comparison between the MAAP and the off-line PP_UniMI polar photometer carried out by Valentini et al. (2020b) pointed to a possible measurement bias of the MAAP absorption coefficients. It is well established that the MAAP, although limited to one measuring wavelength, is the most accurate filter-based on-line method available for the determination of the absorption coefficient (Petzold et al., 2005; Sheridan et al., 2005; Andreae and Gelencsér, 2006; Müller et al., 2011a). Therefore, it is often taken as the reference in inter-comparison exercises with other instruments, such as the AE33 e.g. in Backman et al. (2017). The discrepancy between MAAP and PP_UniMI reported by Valentini et al. (2020b) was mainly attributed to the value of the fraction of backscattered radiation set in the MAAP algorithm and directly measured by PP_UniMI thanks to the high angular resolution which scans the whole scattering plane (resolution of 0.4 degrees in the scattering angle range 0-173°). Valentini et al. (2020b) also reported no differences between MAAP and PP_UniMI when the PP_UniMI was used with the same assumptions as those used in the MAAP (PaM as defined in Valentini et al., 2020b).

The main aim of this study is to characterize the C factor for different filter tapes used in AE33 instruments including the currently used M8060. To do this, we compared the absorption measurements from the off-line PP_UniMI polar photometer with the on-line MAAP and AE33 measurements performed at three measurement stations (urban background, regional background and mountain-top stations) in the Western Mediterranean Basin (WMB). As mentioned, the comparison between PP_UniMI and MAAP was reported in Valentini et al. (2020b) where data from BCN and MSY stations were also used to evaluate the performances of PP_UniMI vs MAAP. One of the objectives of this study is using the multi-wavelength absorption coefficient measurements from the off-line polar photometer extrapolated to the seven AE33 measurement wavelengths to study the wavelength dependence of the AE33 C factor at the three measurement sites. Moreover, the novelty of this study relies also in the fact that we studied the seasonal variations of the C factor and explored its cross-sensitivity to scattering relating it to the physical and optical properties of the collected particles at the three sites. This allowed us to obtain both the multiple scattering parameter, $C_f$, and the cross-sensitivity to scattering, $m_s$, constants for the M8060 filter currently used by the AE33 aethalometers. Moreover, we compared the results for the M8060 filter tape with the previously used TFE-coated glass filter tape (T60A20, also referred to as M8020) (Weingartner et al., 2003; Arnott et al., 2005; Drinovec et al., 2015) for different background scenarios.

## 2 Methodology

### 2.1 Measurement sites

Aerosols measurements were performed at Barcelona (BCN, urban background, $41°23'24.01''$N,$02°6'58.06''$E, 80 m a.s.l.), Montseny (MSY, regional background, $41°46'46''$N, $02°21'29''$E, 720 m a.s.l.) and Montsec (MSA, mountain-top, $42°03'05''$N, $00°43'46''$E, 1570 m a.s.l.) monitoring supersites (NE Spain). As shown later, these measurement stations are characterized by aerosols with different physical and chemical properties that differently influenced the obtained C values. A detailed characterization of the three measurement stations can be found in previous works (e.g. Querol et al. (2001); Rodrıguez et al. (2001);

https://doi.org/10.5194/amt-2021-46
Preprint. Discussion started: 29 March 2021


Atmospheric Measurement Techniques Discussions

Reche et al. (2011); Brines et al. (2014, 2015); Ealo et al. (2018) for BCN; Pérez et al. (2008); Pey et al. (2009); Pandolfi et al. (2011, 2014a, 2016) for MSY; Pandolfi et al. (2014b); Ripoll et al. (2014); Ealo et al. (2016, 2018) for MSA). Briefly, BCN station is located within the Barcelona metropolitan area of nearly 4.5 million inhabitants at a distance of about 5 km from the coast. MSY station is located in a hilly and densely forested area, 50 km to the N–NE of the Barcelona and 25 km from the Mediterranean coast. MSA station is located in a remote high-altitude emplacement in the southern side of the Pre-Pyrenees at the Montsec d'Ares Mountain Range, at 140 km to the NW of Barcelona and 140 km to the WNW of MSY. These super-sites are part of the Catalonian Air Quality Monitoring Network and are part of ACTRIS and GAW networks. Aerosol optical properties at the three sites were measured following standard protocols (WMO/GAW, 2016).

The area of study is characterized by high concentrations of both primary and secondary aerosols, especially in summer (Rodríguez et al., 2002; Dayan et al., 2017; Rivas et al., 2020; Brean et al., 2020) from diverse emission sources. Anthropogenic emissions from road traffic, industry, agriculture, and maritime shipping, among others, strongly contribute to the air quality impairment in this region (Querol et al., 2009b; Amato et al., 2009; Pandolfi et al., 2014c). Moreover, the Mediterranean Basin is also highly influenced by natural sources, such as mineral dust from African deserts and smoke from forest fires (Bergametti et al., 1989; Querol et al., 1998; Rodrıguez et al., 2001; Lyamani et al., 2006; Mona et al., 2006; Koçak et al., 2007; Kalivitis et al., 2007; Querol et al., 2009b; Schauer et al., 2016; Ealo et al., 2016; Querol et al., 2019, among others).

## 2.2 Aerosol characterization

### 2.2.1 Aerosol absorption and eBC measurements

The on-line aerosol absorption coefficient, $b_{abs}$, was measured at the three sites with a multi angle absorption photometer (MAAP, Model 5012, Thermo, Inc., USA, Petzold and Schönlinner, 2004). This instrument derives the absorption coefficient at 637 $\mathrm{nm}$ (Müller et al., 2011a) and eBC concentration using a radiative transfer model from the measurements of transmission of light through the filter tape and backscattering of light at two different angles. eBC and attenuation measurements, $b_{atn}$, were also performed with the AE33 multi-wavelengths aethalometer (model AE33, Magee Scientific, Aerosol d.o.o. Drinovec et al., 2015). The AE33 is based on the measurement at 7 different wavelengths (370, 470, 520, 590, 660, 880, and 950 $\mathrm{nm}$) of the transmission of light through two sample spots with different flows and particle loading relative to the reference spot. It derives the eBC concentration and the attenuation coefficients by applying eqs. (1) and (2), respectively, following Drinovec et al. (2015):

$$eBC = \frac{S \cdot (\Delta \mathrm{ATN}_1/100)}{F_1(1-\zeta) \cdot \sigma_{abs} \cdot C(1-k\Delta \mathrm{ATN}_1) \cdot \Delta t}; \quad (1)$$

$$b_{atn} = \frac{S \cdot (\Delta \mathrm{ATN}_1/100)}{F_1(1-\zeta) \cdot (1-k\Delta \mathrm{ATN}_1) \cdot \Delta t}, \quad (2)$$

where S is the filter surface area loaded with the sample, $\mathrm{F}_1$ the volumetric flow of the spot 1, $\zeta$ the lateral airflow leakage, $\sigma_{abs}$ the mass-absorption cross-section, k the loading factor parameter and $\Delta \mathrm{ATN}_1$ the variation of attenuation of light of the filter tape loaded with the sample of the spot 1, $\mathrm{ATN}_1$, during the measurement timestamp $\Delta t$.

https://doi.org/10.5194/amt-2021-46
Preprint. Discussion started: 29 March 2021


Atmospheric Measurement Techniques Discussions

The Aethalometer absorption coefficient can be derived by dividing the attenuation coefficient (eq. 2) by the multiple scattering parameter C of the filter tape:

$$b_{abs} = \frac{b_{atn}}{C}, \tag{3}$$

Off-line multi-wavelength particle absorption coefficients were obtained using the PP_UniMI polar photometer (Vecchi et al., 2014; Bernardoni et al., 2017) measurements on the MAAP filter spots. 85 filter spots collected at BCN in the period October 2018 - June 2019, 123 filter spots collected at MSY between June - December 2018 (Valentini et al., 2020b), and 121 filter spots collected at MSA between June and November 2018 were analyzed. The PP_UniMI measures the transmitted and scattered radiation at 4 wavelengths (405, 532, 635 and 780 $\mathrm{nm}$) in a range of scattering angles from $0^\circ$ to $173^\circ$ with a resolution down to $0.4^\circ$ and applies a radiative transfer model to derive the absorption coefficients. The PP_UniMI working principle and the detailed analysis of the inter-comparison between the MAAP and PP_UniMI for different measurement sites, including BCN and MSY, was reported in Vecchi et al. (2014); Bernardoni et al. (2017) and in Valentini et al. (2020b). As mentioned before, in these studies no differences were observed between MAAP and PP_UniMI when the latter was used as a MAAP (PaM), i.e. using a data inversion with similar assumptions as those performed in the MAAP.

Here we first obtained the wavelength dependent attenuation coefficients $b_{atn}^{\lambda}$ derived exclusively from the AE33 measurements by multiplying the eBC concentrations provided by the AE33 (eq. 4) by the default wavelength independent instrumental filter value $C_{instr}$ from the AE33 setup file (1.57 for the TFE-coated glass fiber tape T60A20, also referred to as M8020; and 1.39 for the M8060 filter tape),

$$b_{atn}^{\lambda} = eBC^{\lambda} \cdot \sigma_{abs}^{\lambda} \cdot C_{instr}. \tag{4}$$

Then, we determined the average and seasonal multiple scattering factor C both as the ratio between the AE33 attenuation coefficients and the absorption coefficients $b_{abs}^{\lambda}$ measured by the MAAP and the PP_UniMI (eq. 5), and also by applying a Deming regression between the AE33 attenuation coefficients and the MAAP absorption coefficients for the average values for each filter tape.

$$C^{\lambda} = \frac{b_{atn}^{\lambda}}{b_{abs}^{\lambda}} \tag{5}$$

This value of the multiple scattering parameter $C^{\lambda}$ is the value derived from the experimental comparison of different instruments, contrasting the default instrumental constant value $C_{instr}$. The data availability at BCN station ranged between 2016 and 2020, at MSY and MSA data was measured from 2013 to 2020. Different AE33 filter tapes were used during these periods at the three stations as shown in Fig. S1.

#### 2.2.2 Aerosol scattering measurements

On-line particle total scattering ($b_{sp}$) and hemispheric backscatter ($b_{bsp}$) coefficients were measured on-line at the three sites with LED-based integrating nephelometers (Aurora 3000, ECOTECH Pty, Ltd, Knoxfield, Australia) operating at three wavelengths ($450$, $525$ and $635$ $\mathrm{nm}$). Calibration of the nephelometers was performed three times per year using $CO_2$ as span gas

https://doi.org/10.5194/amt-2021-46
Preprint. Discussion started: 29 March 2021


Atmospheric Measurement Techniques Discussions

while zero adjusts were performed once per day using internally filtered particle-free air. The RH threshold was set by using a processor-controlled automatic heater inside the Aurora 3000 nephelometer to ensure a sampling RH of less than 40 % (GAW, 2016). $\sigma_{sp}$ coefficients were corrected for non-ideal illumination of the light source and for truncation of the sensing volumes following the procedure described in Müller et al. (2011b).

## 2.3 Data treatment and conceptual model

The different analyses performed herein were performed considering the absorption coefficients provided either by the MAAP or the PP_UniMI as reference absorption measurements depending on either time resolution and coverage, or on the measurement availability at several wavelengths. The AE33 and MAAP data (provided with high temporal resolution) were used to study the seasonal variations and the cross-sensitivity to scattering of the C factor. The AE33 and PP_UniMI data (provided with low temporal resolution but at different wavelengths) were used to determine the wavelength dependence of the C factor.

### 2.3.1 Average, seasonal values analysis and cross-sensitivity to scattering analysis

As aforementioned, the seasonal analysis of the C factor, its average values and the study of its cross-sensitivity to scattering were performed using the long high-time resolution dataset from the MAAP and AE33 measurements at the three measurement sites. For this, we applied eq. (5) using the absorption coefficient from the MAAP and the AE33 attenuation coefficient extrapolated to the 637 nm wavelength of the MAAP through the Ångström exponent obtained from the AE33 measurements at 7 wavelengths.

The cross-sensitivity to scattering which, as shown later, can strongly affect the C factor values, is neglected in AE33 applications where it is generally assumed that the measured light attenuation is only due to the absorption of light by the collected particles (eqs. 1-2). Moreover, it is also generally assumed that the multiple scattering by particles is sample independent, or constant, and can be taken into account by introducing the multiple scattering correction factor C (Drinovec et al., 2015). However, this assumption is a first approximation, since the attenuation of transmitted light is also due to the scattering of light by the collected particles (Bond et al., 1999; Arnott et al., 2005). Taking this dependence into account and following Arnott et al. (2005), Schmid et al. (2006) and Segura et al. (2014), we parameterized the light attenuation coefficient as:

$$b_{atn} = \frac{S}{F}\frac{\Delta \mathrm{ATN}}{\Delta t} \cdot f(ATN) + m_s \cdot b_{sp} \tag{6}$$

to obtain the relationship between the absorption, attenuation and scattering coefficients:

$$b_{abs} = \frac{b_{atn}}{C_f} - m \cdot b_{sp}\ , \tag{7}$$

where $f(ATN)$ is the function which contains all the dependencies of the measurement shown in eq. (4), i.e. filter loading correction and leakage, and can be assumed to be close 1 (Schmid et al., 2006). The cross-sensitivity to scattering, which is denoted by the constant $\mathrm{m_s}$, is related with $\mathrm{m}$ through $\mathrm{m} = \mathrm{m_s}/\mathrm{C_f}$. Here $\mathrm{C_f}$ refers to the filter multiple scattering parameter, that is a value (possibly wavelength dependent) depending only on filter properties. If we rearrange eq. (7) by expressing the scattering coefficient through the single scattering albedo, we obtain the dependence of the absorption as a function of SSA

https://doi.org/10.5194/amt-2021-46
Preprint. Discussion started: 29 March 2021


Atmospheric Measurement Techniques Discussions

(eq.8). Following eq. 5, we obtain the multiple scattering parameter, $C_f$, but the effective C actually measured, $C_{eff}$, is affected by the cross-sensitivity to the scattering coefficient, as shown in eq. (9).

$$b_{abs} = \frac{b_{atn}}{C_f} \cdot \frac{1}{1 + m \cdot \frac{SSA}{1-SSA}} \tag{8}$$

$$C_{eff} = C_f \left(1 + m \cdot \frac{SSA}{1-SSA}\right) = C_f + m_s \cdot \frac{SSA}{1-SSA} \tag{9}$$

The effective multiple scattering parameter $C_{eff}$ is derived from the comparison of the instruments (AE33, MAAP and nephelometer) and therefore includes the properties of collected particles, and, consequently, also any sensitivity of the measurement to the sample properties other than absorption. The most important cross-sensitivity is due to scattering. The actual AE33 cross-sensitivity to scattering is more pronounced when the measured aerosol particles have higher SSA (eq. 9), whereas for particles with lower SSA it becomes closer to eq. (5).

By analyzing the dependency of the multiple scattering parameter C with the SSA we can obtain the experimental constants of the filter properties $C_f$ and $m_s$. Furthermore, given that the cross-sensitivity to scattering of C depends on the physical and optical (both extensive and intensive) properties of collected particles, we can study its dependency on the shape, size and mixing state of the collected aerosol particles (see Section 3.3 and Supplementary material).

The AE33 data treatment applied to obtain the C seasonality and the cross-sensitivity to scattering included a pre-process filtering method following the approach suggested in Springston and Sedlacek (2007) and Backman et al. (2017). This filtering method consists on setting a threshold value for the measured attenuation variation, $\Delta ATN_1$, high enough so that the signal-to-noise ratio is large; herein we have used a fixed value of 0.01. As can be deduced from eq. (1), the faster the fixed $\Delta ATN_1$ is reached, the shorter is the period $\Delta t$, implying therefore a higher eBC concentration value during the same period. The method we employed determines the period at which the $\Delta ATN_1$ step was reached and recalculated the eBC concentration for this $\Delta t$. As a consequence of this eBC re-calculation, we filtered out the noise resulting from very small values close to the detection limit of the instrument while maintaining the higher eBC values measured without introducing a bias to the measurements as is the case when averaging. With the aim to study the seasonality of the C factor and its cross-sensitivity to scattering, we averaged $b_{abs,MAAP}$ and $b_{sp}$ coefficients to match the corresponding AE33 variable timestamp, $\Delta t$, which ranged approximately between 3 and 14 min (cf. Fig. S2).

### 2.3.2 Wavelength dependence analysis

To study the wavelength dependence of the C factor we compared the absorption coefficients at several wavelengths measured with the PP_UniMI with the attenuation coefficients obtained from the AE33 (eq. 5). Since the off-line PP_UniMI measurements were performed on the MAAP spots, the AE33 attenuation coefficients were averaged over the timestamp of each one of the selected MAAP spots. The absorption coefficients from the PP_UniMI were inter/extrapolated to the seven AE33 wavelengths using the absorption Ångström exponent from the PP_UniMI absorption measurements.

https://doi.org/10.5194/amt-2021-46
Preprint. Discussion started: 29 March 2021


Atmospheric Measurement Techniques Discussions

Valentini et al. (2020b) reported that the MAAP overestimates the absorption coefficient compared to the PP_UniMI. For BCN and MSY Valentini et al. (2020b) reported a MAAP overestimation of 18% and 21%, respectively. By applying the same methodology as in Valentini et al. (2020b) we obtained a difference between MAAP and PP_UniMI for MSA of 19% (Fig. A1) similar to the biases obtained for BCN and MSY. For this reason, Valentini et al. (2020b) also studied the comparison between MAAP and PP_UniMI using for the PP_UniMI data inversion the same assumptions as those performed in the MAAP (PaM approach) and reported a 1:1 correlation between the two instruments. Given that most of the aethalometer C values reported in literature were obtained by comparing AE33 attenuation measurements and MAAP absorption measurements, we report here also the median C values obtained comparing the AE33 with the PP_UniMI (Table S2) and with PaM (Table S3).

## 3 Results

### 3.1 Multiple scattering correction factor: Average values and seasonal variation

Here we present the seasonal cycle of the C factor calculated at 637 nm at BCN, MSY and MSA. For this, we used the AE33 attenuation measurements extrapolated to the MAAP wavelength of 637 nm and divided the attenuation by the absorption measurements provided by the MAAP (eq. 5).

We analyzed the multiple scattering parameter C values through both a Deming regression, taking into account the measurement error of the MAAP (Petzold and Schönlinner, 2004, 12%;) and of the AE33 (15%; Zanatta et al., 2016; Rigler et al., 2020) and by calculating the median value of the C factor as the ratio of the AE33 attenuation coefficient and the MAAP absorption measurements (cf. eq. 5). In the latter case, the uncertainties of the C factor were derived as the half-width at half maximum (HWHM) of the density distribution of the C factor whereas, in the case of the Deming regression, we used the methodological error from the regression slope. The median values of the C factor for the tape M8060 were 2.44 $\pm$ 0.57, 2.23 $\pm$ 0.30, and 2.51 $\pm$ 0.71 for BCN, MSY and MSA, respectively. These values were on average higher compared to the median C values obtained for the TFE-coated glass filter tapes (M8020) of 2.29 $\pm$ 0.48, 2.29 $\pm$ 0.46, 2.36 $\pm$ 0.59 - see Table 1. Figure S3 shows the results of the Deming regression fit between AE33 attenuation ($b_{atn-AE33}$) and MAAP absorption ($b_{abs-MAAP}$) for both the TFE-coated glass and M8060 filter tapes. In Fig. S3 the multiple scattering factor C is the slope of the calculated fits and C values of 1.99 $\pm$ 0.02, 2.05 $\pm$ 0.02, and 2.21 $\pm$ 0.03 (at BCN, MSY and MSA, respectively) were obtained for the TFE-coated glass filter tape whereas slightly higher C values of 2.20 $\pm$ 0.02, 2.13 $\pm$ 0.01, and 2.05 $\pm$ 0.02 were obtained for the M8060 filter tape. We can see from Table 1 that the C values obtained using the median values and the Deming regression were similar, marginally higher for the median method versus the Deming regression, and that both techniques provided higher C factor for the M8060 than for the TFE-coated glass filter tape. The density distribution of the C factor obtained from the ratio (which, as already commented, has a variable time resolution (Sect. 2.3.1), showed a quasi-Gaussian distribution at the three measurement sites with a small tail toward higher C values which could explain the higher values observed using the median compared with the regression. Also, the uncertainties from the Deming regression were lower compared to the uncertainties derived as HWHM of the distributions because the Deming regressions were performed using binned data (cf. Fig. S3).

https://doi.org/10.5194/amt-2021-46
Preprint. Discussion started: 29 March 2021


Atmospheric Measurement Techniques Discussions

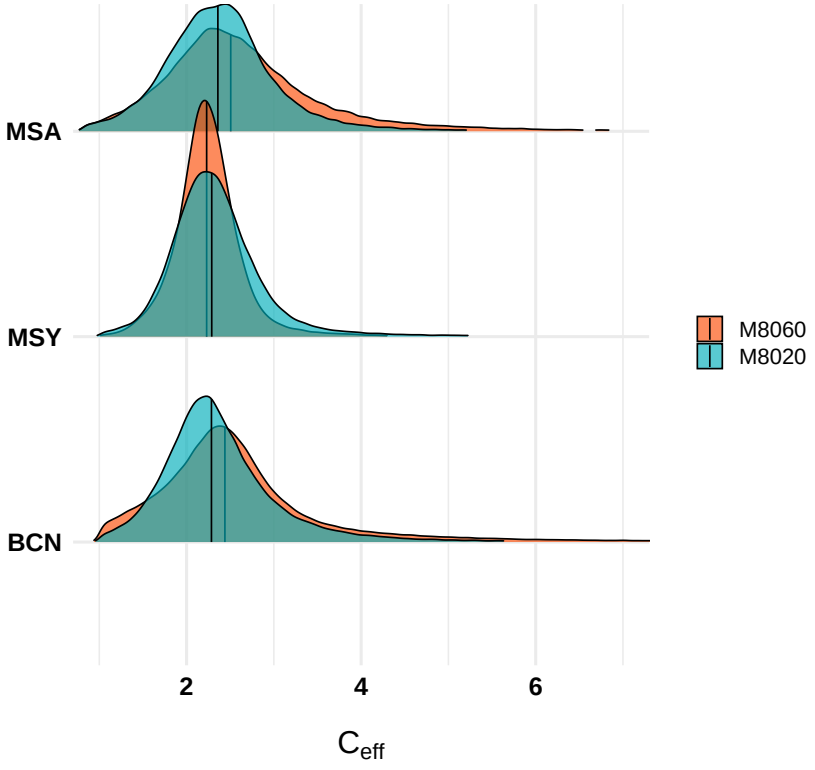


**Figure 1.** Density distribution of the C factor for each filter type, TFE-coated glass (also known as M8020) and M8060, at BCN, MSY, and MSA station. The vertical line represents the median value of each distribution.

The values of the C factor for the AE33 TFE-coated glass and M8060 filter tapes obtained at urban background stations in Rome (Valentini et al., 2020a) and Leipzig (Müller, 2015; Bernardoni et al., 2020) were in the same range as those found in this work for BCN (Table 1).

Figure 2 shows the seasonal variability of the C factor for the TFE-coated glass and M8060 filter tapes at the three stations. Overall, a large variability of the C parameters (cf. Table S1) was observed at the three sites in all seasons, which was coherent with the large range of the C factor values as shown by the density distributions (Fig. 1). This variability was obtained with the described method in section 2.3.1.

An increase of C was observed at MSY and MSA in summer (JJA) for both filter tapes. This increase was likely driven by a greater influence of diurnal processes during the warm months (also in spring (MAM) at MSA) at these two elevated stations and by changes in the chemical and physical properties of collected particles in summer compared to winter (DJF). In fact, spring and summer seasons in the WMB are characterized by a high frequency of Saharan dust outbreaks (e.g. Pey et al., 2013) and formation of high concentrations of secondary organic aerosols and secondary sulfate particles (e.g. Ripoll et al., 2015) which in turn increase the particle scattering efficiency and SSA in summer compared to winter (Pandolfi et al., 2011).

https://doi.org/10.5194/amt-2021-46
Preprint. Discussion started: 29 March 2021


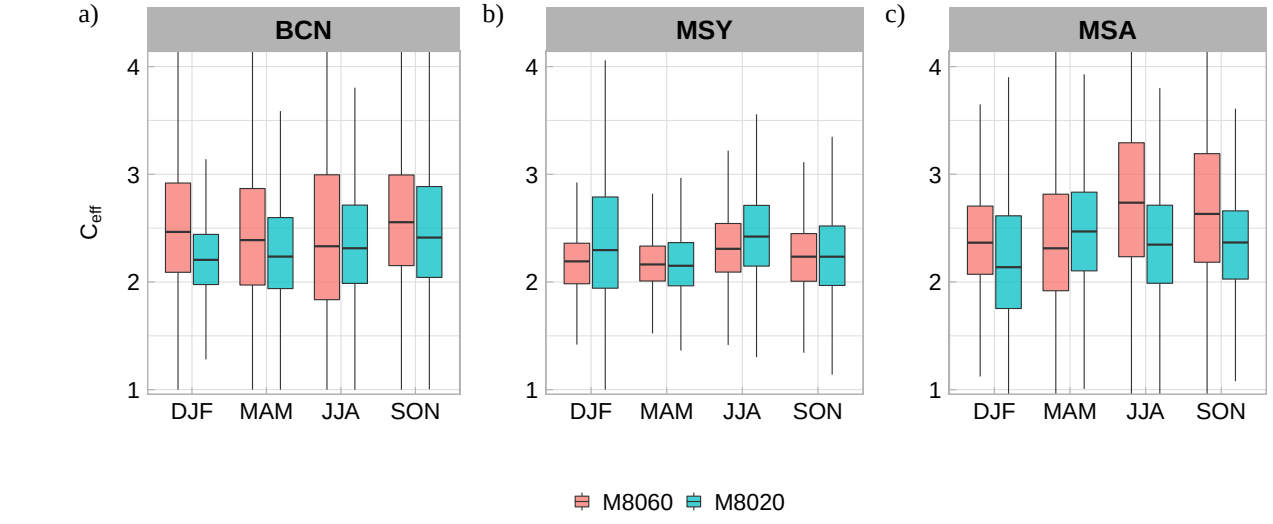


**Figure 2.** Seasonal evolution of the C factor at a) BCN, b) MSY and c) MSA measurement stations for both TFE-coated glass (M8020) and M8060 filter tapes. The box plot boxes show the range between the first and third quartile (IQR) with the median value for each season distribution represented by the inner line; the maximum whisker length is proportional to 1.5 times the third and first quartile difference, or inter-quartile range (1.5 · IQR).

As shown later, high SSA increases the C values above the commonly measured values. In BCN, however, the C remained fairly constant during the different seasons likely because of its greater influence to season-independent local pollutant sources compared to MSY and MSA.

### 3.2 Wavelength dependence analysis from the PP_UniMI vs AE33 comparison

The AE33 $C_{eff}(\lambda)$ factor and its spectral dependence (Fig. 3) was studied at the three stations by comparing the attenuation coefficients, $b_{atn}$ from AE33 at seven different wavelengths with the absorption coefficients, $b_{abs}$, from the PP_UniMI. To this aim, the PP_UniMI absorption coefficients were inter/extrapolated to the seven AE33 wavelengths using the Absorption Ångström Exponent (AAE) obtained from the original PP_UniMI measurements. The obtained mean AAE were $1.12 \pm 0.17$, $1.29 \pm 0.24$, and $1.35 \pm 0.18$ for BCN, MSY, and MSA stations, respectively, with an increase from the urban (BCN) to the remote (MSA) site due to the increase in the relative importance of non-fossil BC sources (i.e. biomass burning) at the remote sites compared to BCN.

At the urban (BCN) and the regional (MSY) stations the C factor did not show any statistically significant dependence with the wavelength (Fig. 3). However, at the remote MSA station the multiple scattering parameter C showed (Fig. 3) a statistically significant increase between 370 ($C_{eff}$=3.47) and 950 nm ($C_{eff}$=4.03) wavelengths (cf. Table S2). The observed increase of the C factor with the wavelength can affect the absorption coefficients derived from the AE33 attenuation measurements and, consequently, can affect parameters such as the absorption Ångström exponent (AAE) or the single scattering albedo

https://doi.org/10.5194/amt-2021-46
Preprint. Discussion started: 29 March 2021


Atmospheric Measurement Techniques Discussions

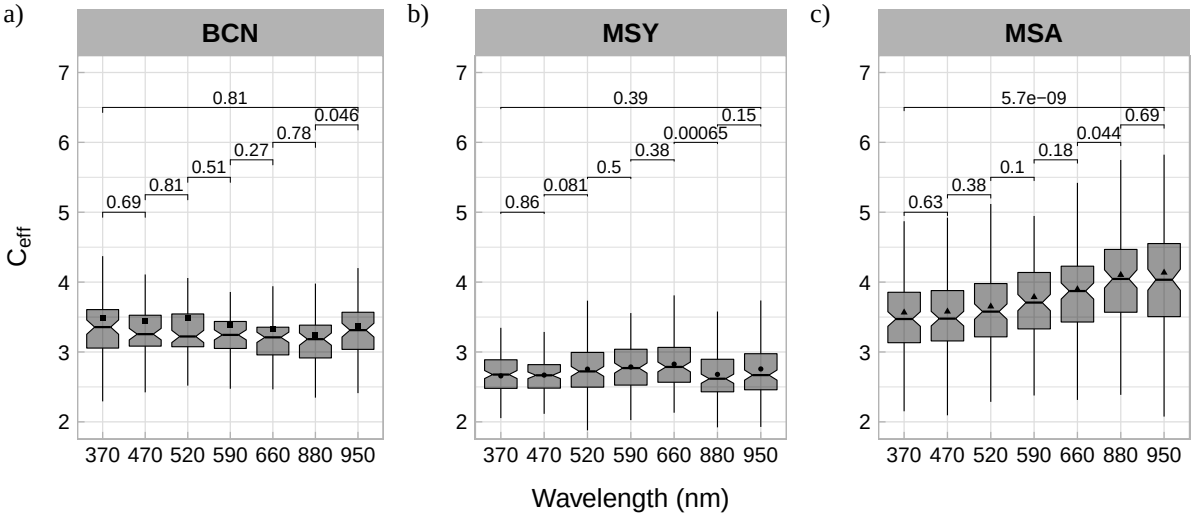


**Figure 3.** Wavelength dependence of C at BCN, MSY and MSA comparing $b_{atn}$ from the AE33 measured at each wavelength and $b_{abs}$ inter/extrapolated to the same wavelength from the PP_UniMI. Box plots have been obtained as in Fig. 2 with the addition of the mean value of the distribution for each wavelength represented by a marker. The values above the box plots between adjacent wavelengths and between 370 and 950 nm wavelength box plots show the obtained p-values, with p<0.05 meaning a statistically significance difference.

(SSA) which can be derived from the multi-wavelengths AE33 absorption measurements. Moreover, a wavelength-dependent C factor can have an impact on aethalometer based BC source apportionment analysis, such as the Aethalometer model, used to determine the contribution from fossil fuels vs biomass burning emissions (Sandradewi et al., 2008). Weingartner et al. (2003) and Segura et al. (2014) found no wavelength dependence for the multiple scattering parameter C for older versions of aethalometer (model AE31), whereas Bernardoni et al. (2020) found a decrease of the C factor with wavelengths, although not statistically significant, and reported the impact of the wavelength dependent C on source apportionment model results.

Virkkula et al. (2015) and Drinovec et al. (2017) have shown that the AE33 factor loading parameter, k, increases with increasing BF (smaller particles) and decreases with increasing SSA and that the wavelength dependence of k also depends on these two optical properties. Moreover, Drinovec et al. (2017) have shown that the BC coating reduces the k at longer wavelengths for higher SSA. Thus, particle size, ageing and BC-coating processes can potentially affect the AE33 factor loading k.

In order to understand the likely reasons causing the observed dependence of the C with wavelength at MSA, we performed a similar analysis as in Virkkula et al. (2015) by comparing the C and its wavelength dependence with different aerosol particles intensive optical properties. Figure 4 shows the wavelength-dependence of the factor C (i.e. the slope of C vs. wavelength, $a_C$) with SSA, BF, and the single-scattering albedo Ångström exponent (SSAAE) at the three sites.

Figure 4 shows no clear relationship of $a_C$ with SSA and BF at BCN and MSY. At MSA, however, Figures 4c,f show that $a_C$ increased with an increasing SSA and decreased with an increasing BF; i.e. variations of BF and SSA can cause the factor

https://doi.org/10.5194/amt-2021-46
Preprint. Discussion started: 29 March 2021


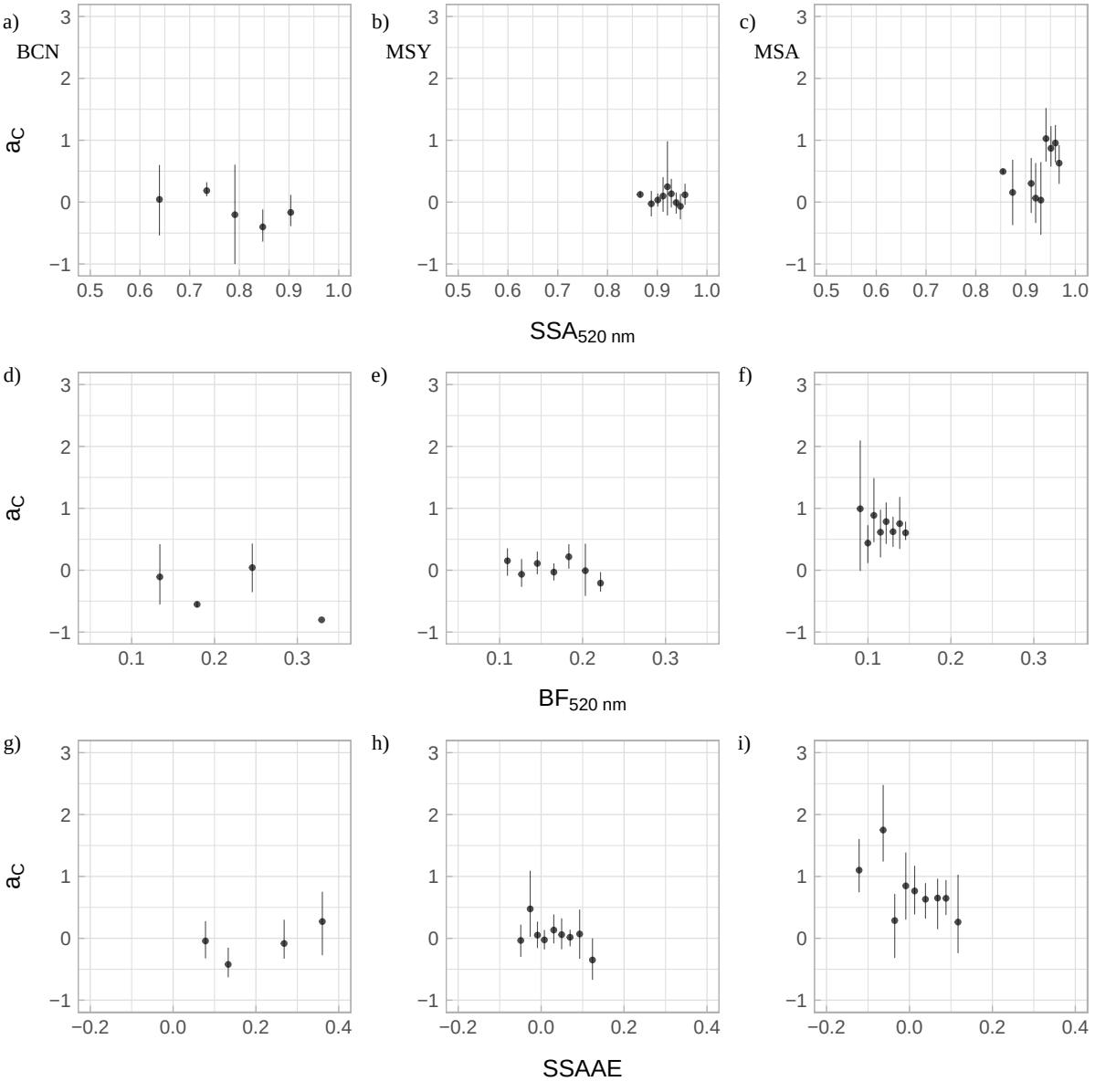


**Figure 4.** Relationship between $a_C$, the slope of the factor C and the wavelength, and the single-scattering albedo at 520 nm ($SSA_{520nm}$), the backscatter fraction ($BF_{520nm}$), and the single-scattering albedo Ångström exponent (SSAAE) at BCN (left panel), MSY (middle panel) and MSA (right panel) measurement stations.

355 C to change as a function of the wavelengths. In Sect. 3.3 we will show (Fig. S9) that high SSA was related to the presence of dust from Saharan deserts (Saharan dust outbreaks). Thus, the increase of C slope with decreasing BF (larger particles) and with increasing SSA at MSA was likely caused by Saharan dust outbreaks affecting the station. To further demonstrate the

https://doi.org/10.5194/amt-2021-46
Preprint. Discussion started: 29 March 2021


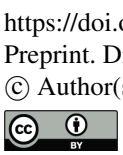

Atmospheric Measurement Techniques Discussions

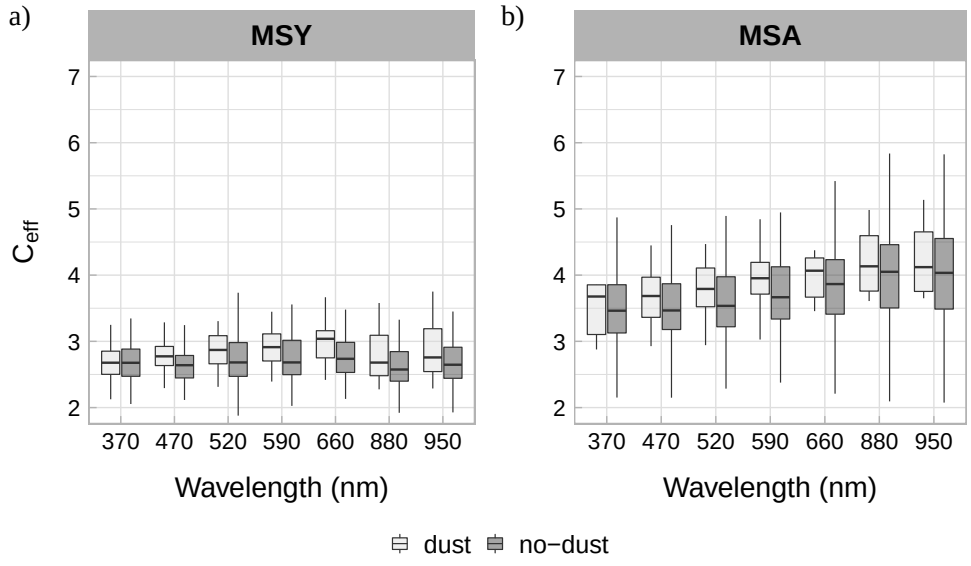


**Figure 5.** Wavelength dependence of C at a) MSY and, b) MSA comparing $b_{atn}$ from the AE33 measured at each wavelength and $b_{abs}$ inter/extrapolated to the same wavelength from the PP_UniMI. Box plots have been obtained as in Fig. 2 and separated into two categories depending whether Saharan dust outbreaks took place (dust) or not (no-dust).

role of dust particles in $a_C$, Fig. 4i shows that the $a_C$ at MSA was the highest when the SSAAE was negative. In fact, negative SSAAE values have been related to the predominance of dust particles in the atmosphere (e.g. Collaud Coen et al., 2010; Ealo et al., 2016). Indeed, Ealo et al. (2016) have shown that the ability of a SSAAE to indicate the presence of dust in the atmosphere strongly depends on the relative importance of fine particles from local sources, and that the SSAAE can detect a higher number of Saharan dust outbreaks at MSA, due to its remote location, compared to MSY where local meteorology (i.e. sea breeze) effectively transports every day fine particles from the urbanized/industrialized coastline where BCN is located. Nevertheless, as shown in Fig. 5b, the comparison between the C factor calculated during days affected by Saharan dust and during days not affected by dust revealed that the slope at MSA remained positive also for no-dust days, suggesting that other particle properties contributed to the positive aC observed at mountain-top station. In addition, Figures 5a,b show that when the MSY and MSA stations were affected by Saharan dust, the factor C increased at all wavelengths compared to non-dust days with a major effect observed at MSA compared to MSY. We will present later in this paper that high SSA determined an increase of the C and that, at the stations considered here, high SSA was always associated to presence of dust from Saharan deserts 3.3.

For the study period considered here, the lack of wavelength-dependence of C at BCN and MSY could be due to the increased relative importance of local anthropogenic particles at these stations compared to MSA during Saharan dust outbreaks (Pandolfi et al., 2014b). Furthermore, Figs. 4g,h show that (based on the data available in this work) the SSAAE was positive at BCN and slightly negative at MSY keeping positive values for the majority of the analyzed samples. Thus, we hypothesize that at

https://doi.org/10.5194/amt-2021-46
Preprint. Discussion started: 29 March 2021


Atmospheric Measurement Techniques Discussions

MSA the increase in the relevance of dust particles during Saharan dust outbreaks had a larger effect (compared to MSY and BCN) on the wavelength dependence of the C factor. However. as already noted (Fig. 4i), the slope of the C factor at MSA was the highest when SSAAE was strongly negative but kept positive values also when SSAAE was higher than zero suggesting that dust particles may not be the only reason for the observed increase of C with the wavelength at MSA.

For completeness, we present in the following the dependence of the k factor and its slope with the wavelength ($a_k$) with BF and SSA as done by Virkkula et al. (2015). Since the wavelength dependence of k is intrinsic to the AE33 instrument, for the sake of the analysis we have used the largest dataset at our disposal (Fig. S1), following the data processing mentioned in Sect.2.3.1. As shown in Fig. S4, $a_k$ was negative (i.e. the k decreased with increasing wavelength) for SSA values higher than 0.5, 0.75 and 0.85 at BCN, MSY and MSA, respectively. The relationship between k and SSA (inset graphs in Fig. S4) was similar to that between $a_k$ and SSA. A decrease of $a_k$ with increasing SSA has been also reported by Virkkula et al. (2015) for an urban environment in China (Nanjing). Fig. S4 implies that for darker aerosols, the factor loading correction increases with wavelength, and that, at higher SSA, k decreases with wavelength. Furthermore, at BCN the $a_k$ increased with BF and kept negative values (i.e. the correction decreased with increasing wavelength) up to a BF of 0.2; thereafter, for very fine particles (i.e. BF>0.2) the slope of k became positive, indicating that the correction increased with wavelength. Virkkula et al. (2015) also reported an increase of $a_k$ with increasing BF in Nanjing urban environment; however the $a_k$ was positive starting from BF values higher than 0.14. At MSY and MSA the $a_k$ was always negative (i.e. the correction decreased with increasing wavelength) even if the relationship between $a_k$ (and k) and BF at MSY and MSA was not linear as observed for BCN.

Figure 6 shows the results of the sensitivity study on the effects that the wavelength-dependent C ($C(\lambda)$) had on the calculated AAE compared to the approach based on the application of a constant C factor ($C_{const}$) for all AE33 wavelengths. For BCN and MSY measurement stations, the AAE values did not show any significant variation (cf. Table S4) with mean values of $1.19 \pm 0.15$ and $1.27 \pm 0.12$ (at BCN and MSY, respectively) using a constant C and slightly decreasing to $1.17 \pm 0.15$ and $1.25 \pm 0.12$ (for BCN and MSY, respectively) when the wavelength-dependent C was used. At MSA, the observed increase of the C with the wavelength caused the AAE to increase by 13% from $1.19 \pm 0.07$ (constant C) to $1.35 \pm 0.07$ (wavelength-dependent C). Similarly to the above sensitivity study on the calculated AAE, Fig. S5 reports the SSA calculated using the wavelength-dependent C factor in comparison with the SSA obtained using the constant C factor at 470, 660 and 950 nm. As reported in Fig. S5, a statistically significant increase of the SSA at MSA station of around 1.3% for 660 nm, 2% for 950 nm was observed when using the wavelength-dependent C compared to a constant C. This increase, although not large, is relevant since it occurs at the threshold of SSA value for which a substantial increase of the C as a function of SSA was observed, as shown in Section 3.3. As for the AAE, Fig. S5 shows no significant variation for the SSA values at the 3 wavelengths at BCN and MSY consistent with the observed lack of dependence of the C factor with wavelength.

### 3.3 Multiple scattering parameter cross-sensitivity to scattering

The cross-sensitivity to scattering of the C factor at the three stations was obtained by analyzing the relationship between the multiple scattering parameter $C_{eff}$ (at 637 nm) and SSA.

https://doi.org/10.5194/amt-2021-46
Preprint. Discussion started: 29 March 2021


Atmospheric Measurement Techniques Discussions

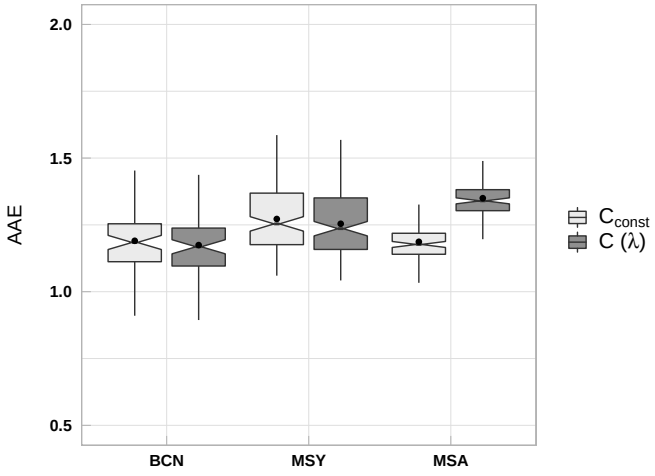


**Figure 6.** The absorption Ångström exponent (AAE) calculated with a constant $C_{const}$ and the wavelength-dependent C(λ) for all stations. Box plots have been obtained as in Figs. 2 and 3, with the markers indicating the mean AAE values.

SSA was obtained independently at 637 $\mathrm{nm}$ using simultaneous MAAP and nephelometer data. $C_{\mathrm{eff}}$ was obtained through eq. (5) using the AE33 attenuation coefficient extrapolated at 637 nm using the AAE from AE33 and the MAAP absorption coefficients at 637 nm. The analysis was performed with SSA measurements binned using Freedman and Diaconis (1981) criteria, and with the average $C_{\mathrm{eff}}$ obtained for each bin. The fit of the binned multiple scattering parameter (eq. 5) following eq. (9) yields the experimental values of both $C_{\mathrm{f}}$ and $m_{\mathrm{s}}$.

Figure 7c and Table 1 show the results of the fit for BCN, MSY and MSA for both filter tapes: the TFE-coated glass filter tape (M8020) and the currently distributed M8060 filter tape. For the TFE-coated glass filter tape, it was found a constant of 2.21 $\pm$ 0.01 and a cross-sensitivity to scattering of 1.8 $\pm$ 0.1 at MSY, and of 1.96 $\pm$ 0.02 and 3.4 $\pm$ 0.1 % for $C_f$ and $m_s$, respectively, at MSA. For the M8060 filter tape, the fit yields a multiple scattering constant $C_f$ of 2.50 $\pm$ 0.02 and a cross-sensitivity to scattering of 1.6 $\pm$ 0.3 % at BCN, a $C_f$ of 1.96 $\pm$ 0.01 and a $m_s$ of 3.0 $\pm$ 0.1 % at MSY, and a constant $C_f$ of 1.82 $\pm$ 0.02 and a $m_s$ 4.9 $\pm$ 0.1 % at MSA.

As a consequence of the cross-sensitivity to scattering we can appreciate in Fig. 7a, 7b, 7d, and 7e an up to 3-fold increase of C for SSA>0.95. This significant increase of the C factor at high SSA, if not accounted for, can lead to a large overestimation of both the eBC concentrations and the absorption coefficients. This effect can have a larger impact at sites where very high SSA values are typically observed as remote arctic sites, mountain-top sites, or sites where aerosol is dominated by mineral dust, among others (Collaud Coen et al., 2004; Pandolfi et al., 2014b, 2018), as well as in places where there are trends of increasing or decreasing SSA (Collaud Coen et al., 2020). This cross-sensitivity to scattering of the filter explains the higher C factors obtained on average at these types of sites (Table 1) and suggests the need of using either a site-specific C, or a C

https://doi.org/10.5194/amt-2021-46
Preprint. Discussion started: 29 March 2021


Atmospheric Measurement Techniques Discussions

**Table 1.** AE33 multiple scattering parameter C for some measurement stations (included BCN, MSY and MSA) and cross-sensitivity to scattering for BCN, MSY and MSA station compared to literature values for AE33 TFE-coated glass (M8020, TFE in the table). Different approaches, as explained in Section 3.1, have been used to obtain the factor C.

| Site | Characteristics | Filter type | Reference | C | $C_{Deming}$ | $C_f$ | $m_s$ (%) |
|---|---|---|---|---|---|---|---|
| **Barcelona** | Urban background | TFE | This study | **2.29 ± 0.49** | **1.99± 0.02** | - | - |
| | | M8060 | This study | **2.44 ± 0.57** | **2.20 ± 0.02** | **2.50 ± 0.02** | **1.6 ± 0.3** |
| Leipzig | Urban background | TFE | Müller (2015) | 3.2 | | | |
| | | TFE | Bernardoni et al. (2020) | | 2.78 | | |
| Rome | Urban background | M8060 | Valentini et al. (2020a) | 2.66 | | | |
| Klagenfurt | Urban background | TFE | Drinovec et al. (2020) | 1.57 | | | |
| **Montseny** | Regional background | TFE | This study | **2.29 ± 0.46** | **2.05 ± 0.02** | **2.21 ± 0.01** | **1.8 ± 0.1** |
| | | M8060 | This study | **2.23 ± 0.30** | **2.13 ± 0.01** | **1.96 ± 0.01** | **3.0 ± 0.1** |
| **Montsec d'Ares** | Mountain-top | TFE | This study | **2.36 ± 0.59** | **2.21 ± 0.03** | **1.96 ± 0.02** | **3.4 ± 0.1** |
| | | M8060 | This study | **2.51 ± 0.71** | **2.05 ± 0.02** | **1.82 ± 0.02** | **4.9 ± 0.1** |
| Mt. Bachelor | Mountain-top | TFE | Laing et al. (2020) | 4.24 | | | |

that takes into account the SSA measured by an independent absorption method. This effect needs to be taken into account for climate studies.

We interpreted the differences in the obtained $C_f$ and $m_s$ values as variations dependent on other sample properties. Size distribution and the mixing state are the most obvious. We studied the dependence of the cross-sensitivity to scattering obtained at BCN, MSY and MSA on different optical parameters (Fig. S6, S7, S8 and S9). We found that the large C values at high SSA were mostly obtained when the sampled aerosol composition was dominated by mineral dust (such as during Saharan dust outbreaks) as demonstrated by the negative Ångström exponent of the SSA (SSAAE) at high SSA. Thus, in prior studies, negative values of the SSAAE have been associated with an aerosol mixture dominated by mineral dust (Collaud Coen et al., 2004; Ealo et al., 2016; Yus-Díez et al., 2020). Moreover, we have found AAE values higher than 1.5 above a SSA of 0.95 (Fig. S6), thus implying a relatively higher absorption fraction in the UV range whether by dust absorbing particles or by BrC aerosols (Kirchstetter et al., 2004b; Chen and Bond, 2010; Zotter et al., 2017; Forello et al., 2019, 2020). Furthermore, we have found, as already mentioned in Sect. 3.2, different behaviour of the C and the factor loading,k, at MSA versus BCN and MSY; Fig. S7, S8, S9 show an increase of the C factor with increasing SSA, decreasing BF, and a SSAAE<0, which can be related to the larger relevance of absorbing dust particles. Fig. S7 and S8 shows that at BCN, while the BF remains constant with an increasing SSA, k decreases, yet the C factor does not show a great increase. This description for our set of sites is coherent with the different aerosol sources, especially the common Saharan dust outbreaks affecting the WMB (Escudero et al., 2005; Querol et al., 2004, 2009b, a; Ealo et al., 2016; Querol et al., 2019; Yus-Díez et al., 2020).

https://doi.org/10.5194/amt-2021-46
Preprint. Discussion started: 29 March 2021


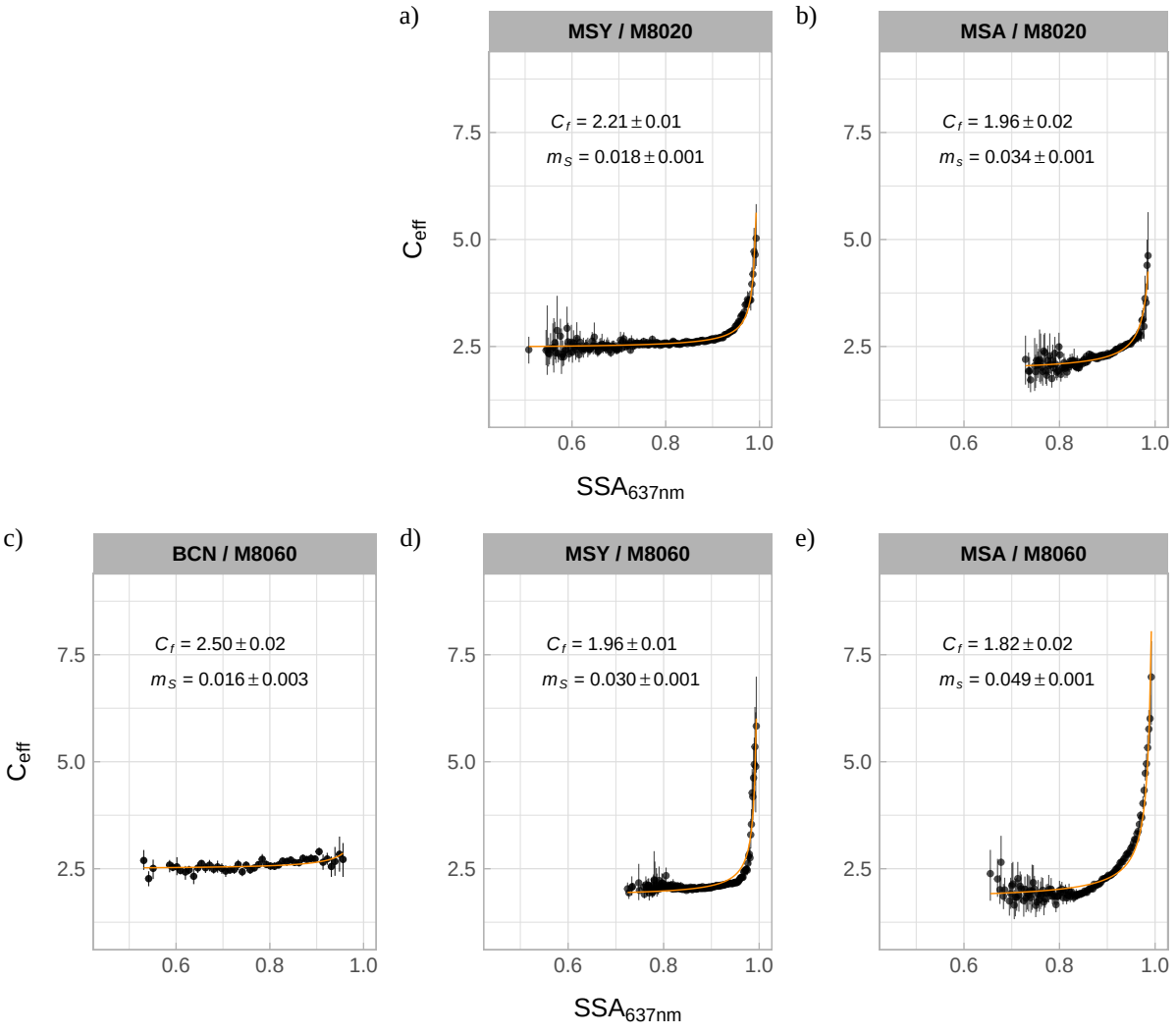


**Figure 7.** Cross-sensitivity to scattering analysis for TFE-coated glass tape (also known as M8020, upper panel) and M8060 filter tape (lower panel) for BCN (c), MSY (a,d) and MSA (b,e) stations obtained by attenuation coefficients from the AE33, absorption coefficients from the MAAP photometer and scattering coefficients from the integrating nephelometer. Each data point represents the mean, and the vertical bars the first and third quartile for each bin. Multiple scattering constant, $C_f$ and cross-sensitivity to scattering, $m_s$, are determined by fitting eq. (9) to the binned data.

## 4 Conclusions

The multiple scattering parameter C for the AE33 dual-spot aethalometer using different tapes materials, the previously used TFE-coated glass and the currently used M8060 filter tapes, has been analyzed using data collected at three different background stations in NE Spain: an urban background station in Barcelona, BCN, a regional background station at Montseny,

https://doi.org/10.5194/amt-2021-46
Preprint. Discussion started: 29 March 2021


Atmospheric Measurement Techniques Discussions

MSY, and a mountain-top station at Montsec d'Ares, MSA. We obtained the C correction factor comparing the AE33 attenuation coefficient measurements with the absorption coefficients measured by a MAAP and used simultaneous scattering measurements from an integrating nephelometer for analyzing the cross-sensitivity to scattering. Moreover, we analyzed the C wavelength dependence at the three sites comparing the AE33 attenuation coefficient measurements with the multi-wavelength PP_UniMI absorption coefficients.

We have found an average multiple scattering parameter C at 637 nm of 2.29, 2.29, 2.36 for the TFE-coated glass filter tape (M8020) and of 2.44, 2.23 and 2.51 for the M8060 filter tape, for BCN, MSY and MSA measurement stations, respectively. The obtained C factor showed a seasonal variability at MSY and MSA with a maximum at summer due to the changes in the physical-chemical aerosol properties. A larger fraction of dust particles and formation of secondary organic aerosols and secondary sulfates likely explained the observed increase of C in summer. However, at the urban background station of BCN the values remain fairly constant throughout the year.

We also analyzed the wavelength dependence of C for the M8060 filter tape for BCN, MSY and MSA. We found a statistically significant increase with the wavelength, from 3.47 for 370 nm to 4.03 for 950 nm for the mountain-top station of MSA, whereas at BCN an MSY background stations no statistically significant dependence was found. The wavelength-dependence of C at the mountain station was in part due to the predominance of dust particles during Saharan dust outbreaks at this station. We also investigated the effect of considering a wavelength-dependent C at MSA station compared with a constant C on the absorption Ångström exponent (AAE) and the single scattering albedo (SSA) through sensitivity tests. Results revealed an increase of the AAE by 13% and an increase of the SSA by 1.3% when using the wavelength-dependent C factor compared to using a constant C factor (i.e. with no $\lambda$–dependence). This effect may impact any source apportionment method which takes into account the multi-wavelength absorption values from the AE33 (e.g. the Aethalometer model). Furthermore, although no statistically significant difference with wavelength was found for the C factor for BCN and MSY, using a wavelength-dependent C instead of a constant one has the potential of modifying the results from the derived intensive optical properties and source apportionment models.

We presented a novel approach for analyzing the cross-sensitivity to scattering of the C correction factor. This approach consisted in fitting the measurements of the C versus SSA. The fits provided the constant $C_f$ and a cross-sensitivity factor $m_S$. We have applied the fits to the TFE-coated glass filter tape at MSY and MSA and we obtained similar results for the cross-sensitivity factor (1.8±0.1% and 3.4±0.1%, respectively) compared to those reported in the literature (around 1-1.5 %). For the first time here we characterized the cross-sensitivity to scattering also of the new M8060 filter tape. We obtained a cross-sensitivity to scattering for the M8060 of 1.6±0.3%, 3.0±0.1% and 4.9±0.1% for BCN, MSY and MSA, respectively. The multiple scattering parameter, $C_f$ for each station and filter tape obtained from the fit for the TFE-coated glass filter tape is $C_f = 2.21 \pm 0.01$ at MSY, and $C_f = 1.96 \pm 0.02$ at MSA. The M8060 filter tape values are: $C_f = 2.50 \pm 0.02$ at BCN, $C_f = 1.96 \pm 0.01$ at MSY, and $C_f = 1.82 \pm 0.02$ at MSA. The consequence of this cross-sensitivity to scattering is the large increase of the C values, up to 3-fold, for SSA values above 0.9-0.95. As a result of this large increase, actual absorption coefficients and eBC concentrations are much lower than those reported by the AE33 when the aerosol particles measured have

https://doi.org/10.5194/amt-2021-46
Preprint. Discussion started: 29 March 2021


Atmospheric Measurement Techniques Discussions

a high SSA (e.g. aged particles, desert dust particle outbreaks, etc.). The effect of this cross-sensitivity to scattering pattern of C is responsible for the higher C values measured at mountain-top and Arctic measurement stations.

The methodology of this study for the C correction factor analysis is of great importance for the retrieval of more accurate aerosol absorption coefficients and equivalent black carbon concentrations at several wavelengths from AE33 instruments. With the approach presented here, the wavelength dependence of the C factor and its cross-sensitivity to scattering can be derived. The C values obtained in this work for different station types (urban, regional, remote) may serve as reference for similar background measurement sites where the same methodology cannot be applied. Yet, discrepancies may arise due to the possible differences in aerosol sources at different sites and, accordingly, to the different aerosol particles compositions and mixing states. Similar analysis for other measurement sites with similar features may reduce the uncertainties around the applicability of the results presented here to other stations.

## Appendix A: Absorption coefficient relationship between a MAAP and a PP_UniMI polar photometer for MSA station

This appendix aims to show the result of applying the same methodology as in Section 3.1 of Valentini et al. (2020b) to the PP_UniMI analyzed dataset for obtaining the bias for the MSA station in the absorption coefficient measurements between the MAAP and the PP_UniMI polar photometer A1. It consists on the application of a Deming regression fit, which results in a slope of $0.81 \pm 0.01$ for our dataset.

*Code and data availability.* The Montseny and Montsec data sets used for this publication are accessible online on the WDCA (World Data Centre for Aerosols) web page: http://ebas.nilu.no. The Barcelona data sets were collected within different national and regional projects and/or agreements and are available upon request. The code used for analysis can be obtained upon request to the corresponding author.

*Author contributions.* DC, SV, RV and VB performed and analyzed the measurements with the PP_UniMI polar photometer. NP, CR, MP, AA and JYD carried out the maintenance and supervision of the BCN, MSY and MSA supersites. AA, GM, MP and XQ played a crucial role in the processes of shaping the manuscript structure as well as helping with the data analysis. JYD developed the data process, the analysis of the results, and summarized and expressed them in this manuscript. All authors provided advice regarding the manuscript structure and content as well as contributed to the writing of the final manuscript.

*Competing interests.* At the time of the research, MR and MI were also employed by the manufacturer of the Aethalometer AE33.

https://doi.org/10.5194/amt-2021-46
Preprint. Discussion started: 29 March 2021


Atmospheric Measurement Techniques Discussions

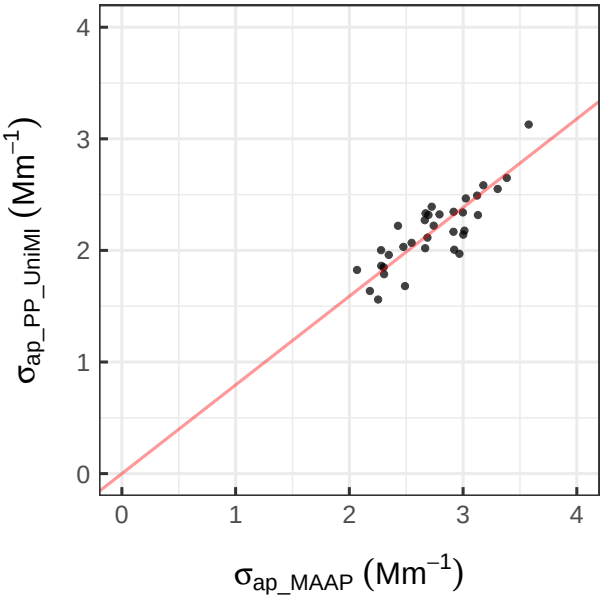


**Figure A1.** Comparison between the aerosol absorption coefficient measured by PP_UniMI on sample spots ($\sigma_{ap\_PP\_UniMI}$) and the MAAP photometer ($\sigma_{ap\_MAAP}$).

*Acknowledgements.* Measurements at Spanish sites (Barcelona, Montseny and Montsec d'Ares) were supported by the Spanish Ministry of Economy, Industry and Competitiveness and I+D+I "Retos Colaboración" funds under the CAIAC project (PID2019-108990PB-100), by the Generalitat de Catalunya (AGAUR 2017 SGR41 and the DGQA) and the European Commission via ACTRIS-IMP (project 871115). We acknowledge support of the COST Action CA16109 COLOSSAL. GM acknowledges support from the Slovenian Research Agency program P1-0385 "Remote sensing of atmospheric properties". IDAEA-CSIC is a Centre of Excellence Severo Ochoa (Spanish Ministry of Science and Innovation, Project CEX2018-000794-S).

https://doi.org/10.5194/amt-2021-46
Preprint. Discussion started: 29 March 2021




## References

Ajtai, T., Filep, Á., Schnaiter, M., Linke, C., Vragel, M., Bozóki, Z. Á., Szabó, G., and Leisner, T.: A novel multi-wavelength photoacoustic spectrometer for the measurement of the UV-vis-NIR spectral absorption coefficient of atmospheric aerosols, Journal of Aerosol Science, 41, 1020–1029, https://doi.org/10.1016/j.jaerosci.2010.07.008, 2010.

Alfaro, S., Lafon, S., Rajot, J., Formenti, P., Gaudichet, A., and Maille, M.: Iron oxides and light absorption by pure desert dust: An experimental study, Journal of Geophysical Research: Atmospheres, 109, 2004.

Amato, F., Querol, X., Alastuey, A., Pandolfi, M., Moreno, T., Gracia, J., and Rodriguez, P.: Evaluating urban PM10 pollution benefit induced by street cleaning activities, Atmospheric Environment, 43, 4472–4480, 2009.

Andreae, M. O. and Gelencsér, A.: Black carbon or brown carbon? the nature of light-absorbing carbonaceous aerosols, Atmospheric Chemistry and Physics, 6, 3131–3148, https://doi.org/10.5194/acp-6-3131-2006, 2006.

Arnott, W. P., Hamasha, K., Moosmüller, H., Sheridan, P. J., and Ogren, J. A.: Towards aerosol light-absorption measurements with a 7-wavelength aethalometer: Evaluation with a photoacoustic instrument and 3-wavelength nephelometer, Aerosol Science and Technology, 39, 17–29, https://doi.org/10.1080/027868290901972, 2005.

Backman, J., Schmeisser, L., Virkkula, A., Ogren, J. A., Asmi, E., Starkweather, S., Sharma, S., Eleftheriadis, K., Uttal, T., Jefferson, A., Bergin, M., Makshtas, A., Tunved, P., and Fiebig, M.: On Aethalometer measurement uncertainties and an instrument correction factor for the Arctic, Atmospheric Measurement Techniques, 10, 5039–5062, https://doi.org/10.5194/amt-10-5039-2017, 2017.

Bergametti, G., Dutot, A.-L., Buat-Menard, P., Losno, R., and Remoudaki, E.: Seasonal variability of the elemental composition of atmospheric aerosol particles over the northwestern Mediterranean, Tellus B: Chemical and Physical Meteorology, 41, 353–361, 1989.

Bergstrom, R. W., Pilewskie, P., Russell, P. B., Redemann, J., Bond, T. C., Quinn, P. K., and Sierau, B.: Spectral absorption properties of atmospheric aerosols, Atmospheric Chemistry and Physics, 7, 5937–5943, https://doi.org/10.5194/acp-7-5937-2007, 2007.

Bernardoni, V., Valli, G., and Vecchi, R.: Set-up of a multi wavelength polar photometer for off-line absorption coefficient measurements on 1-h resolved aerosol samples, Journal of Aerosol Science, 107, 84 – 93, https://doi.org/https://doi.org/10.1016/j.jaerosci.2017.02.009, http://www.sciencedirect.com/science/article/pii/S0021850216301549, 2017.

Bernardoni, V., Ferrero, L., Bolzacchini, E., Forello, A. C., Gregori, A., Mo, G., Prati, P., Rigler, M., Santagostini, L., Soldan, F., Valli, G., and Vecchi, R.: Determination of Aethalometer multiple-scattering enhancement parameters and impact on source apportionment during the winter 2017-2018 EMEP / ACTRIS / COLOSSAL campaign in Milan ., 2020.

Bond, T. C., Anderson, T. L., and Campbell, D.: Calibration and Intercomparison of Filter-Based Measurements of Visible Light Absorption by Aerosols, Aerosol Science and Technology, 30, 582–600, https://doi.org/10.1080/027868299304435, 1999.

Bond, T. C., Doherty, S. J., Fahey, D., Forster, P., Berntsen, T., DeAngelo, B., Flanner, M., Ghan, S., Kärcher, B., Koch, D., et al.: Bounding the role of black carbon in the climate system: A scientific assessment, Journal of Geophysical Research: Atmospheres, 118, 5380–5552, 2013.

Brean, J., Beddows, D., Shi, Z., Temime-Roussel, B., Marchand, N., Querol, X., Alastuey, A., Minguillón, M. C., and Harrison, R. M.: Molecular insights into new particle formation in Barcelona, Spain, Atmospheric Chemistry and Physics, 20, 10 029–10 045, 2020.

Brines, M., Dall'Osto, M., Beddows, D. C., Harrison, R. M., and Querol, X.: Simplifying aerosol size distributions modes simultaneously detected at four monitoring sites during SAPUSS, Atmospheric Chemistry and Physics, 14, 2973–2986, https://doi.org/10.5194/acp-14-2973-2014, 2014.

https://doi.org/10.5194/amt-2021-46
Preprint. Discussion started: 29 March 2021




Brines, M., Dall'Osto, M., Beddows, D. C., Harrison, R. M., Gómez-Moreno, F., Núñez, L., Artíñano, B., Costabile, F., Gobbi, G. P., Salimi, F., Morawska, L., Sioutas, C., and Querol, X.: Traffic and nucleation events as main sources of ultrafine particles in high-insolation developed world cities, Atmospheric Chemistry and Physics, 15, 5929–5945, https://doi.org/10.5194/acp-15-5929-2015, 2015.

Cappa, C. D., Zhang, X., Russell, L. M., Collier, S., Lee, A. K., Chen, C. L., Betha, R., Chen, S., Liu, J., Price, D. J., Sanchez, K. J., McMeeking, G. R., Williams, L. R., Onasch, T. B., Worsnop, D. R., Abbatt, J., and Zhang, Q.: Light Absorption by Ambient Black and Brown Carbon and its Dependence on Black Carbon Coating State for Two California, USA, Cities in Winter and Summer, Journal of Geophysical Research: Atmospheres, 124, 1550–1577, https://doi.org/10.1029/2018JD029501, 2019.

Chen, Y. and Bond, T. C.: Light absorption by organic carbon from wood combustion., Atmospheric Chemistry & Physics, 10, 2010.

Collaud Coen, M., Weingartner, E., Schaub, D., Hueglin, C., Corrigan, C., Henning, S., Schwikowski, M., and Baltensperger, U.: Saharan dust events at the Jungfraujoch: detection by wavelength dependence of the single scattering albedo and first climatology analysis, pp. 2465–2480, 2004.

Collaud Coen, M., Weingartner, E., Apituley, A., Ceburnis, D., Fierz-Schmidhauser, R., Flentje, H., Henzing, J. S., Jennings, S. G., Moerman, M., Petzold, A., Schmid, O., and Baltensperger, U.: Minimizing light absorption measurement artifacts of the Aethalometer: Evaluation of five correction algorithms, Atmospheric Measurement Techniques, 3, 457–474, https://doi.org/10.5194/amt-3-457-2010, 2010.

Collaud Coen, M., Andrews, E., Lastuey, A., Petkov Arsov, T., Backman, J., Brem, B. T., Bukowiecki, N., Couret, C., Eleftheriadis, K., Flentje, H., Fiebig, M., Gysel-Beer, M., Hand, J. L., Hoffer, A., Hooda, R., Hueglin, C., Joubert, W., Keywood, M., Eun Kim, J., Kim, S. W., Labuschagne, C., Lin, N. H., Lin, Y., Lund Myhre, C., Luoma, K., Lyamani, H., Marinoni, A., Mayol-Bracero, O. L., Mihalopoulos, N., Pandolfi, M., Prats, N., Prenni, A. J., Putaud, J. P., Ries, L., Reisen, F., Sellegri, K., Sharma, S., Sheridan, P., Patrick Sherman, J., Sun, J., Titos, G., Torres, E., Tuch, T., Weller, R., Wiedensohler, A., Zieger, P., and Laj, P.: Multidecadal trend analysis of in situ aerosol radiative properties around the world, Atmospheric Chemistry and Physics, 20, 8867–8908, https://doi.org/10.5194/acp-20-8867-2020, 2020.

Corbin, J. C., Pieber, S. M., Czech, H., Zanatta, M., Jakobi, G., Massabò, D., Orasche, J., El Haddad, I., Mensah, A. A., Stengel, B., Drinovec, L., Mocnik, G., Zimmermann, R., Prévôt, A. S., and Gysel, M.: Brown and Black Carbon Emitted by a Marine Engine Operated on Heavy Fuel Oil and Distillate Fuels: Optical Properties, Size Distributions, and Emission Factors, Journal of Geophysical Research: Atmospheres, 123, 6175–6195, https://doi.org/10.1029/2017JD027818, 2018.

Dayan, U., Ricaud, P., Zbinden, R., and Dulac, F.: Atmospheric pollution over the eastern Mediterranean during summer–a review, Atmospheric Chemistry and Physics, 17, 13 233, 2017.

Drinovec, L., Močnik, G., Zotter, P., Prévôt, A., Ruckstuhl, C., Coz, E., Rupakheti, M., Sciare, J., Müller, T., Wiedensohler, A., and Hansen, A. D. A.: The "dual-spot" Aethalometer: an improved measurement of aerosol black carbon with real-time loading compensation, Atmospheric Measurement Techniques, 8, 1965–1979, 2015.

Drinovec, L., Gregoric, A., Zotter, P., Wolf, R., Anne Bruns, E., Bruns, E. A., Prevot, A. S., Favez, O., Sciare, J., Arnold, I. J., Chakrabarty, R. K., Moosmüller, H., Filep, A., and Mocnik, G.: The filter-loading effect by ambient aerosols in filter absorption photometers depends on the coating of the sampled particles, Atmospheric Measurement Techniques, 10, 1043–1059, https://doi.org/10.5194/amt-10-1043-2017, 2017.

Drinovec, L., Sciare, J., Stavroulas, I., Bezantakos, S., Pikridas, M., Unga, F., Savvides, C., Višić, B., Remškar, M., and Močnik, G.: A new optical-based technique for real-time measurements of mineral dust concentration in PM10 using a virtual impactor, Atmospheric Measurement Techniques Discussions, 2, 1–19, https://doi.org/10.5194/amt-2019-506, 2020.

https://doi.org/10.5194/amt-2021-46
Preprint. Discussion started: 29 March 2021




Ealo, M., Alastuey, A., Ripoll, A., Pérez, N., Minguillón, M. C., Querol, X., and Pandolfi, M.: Detection of Saharan dust and biomass burning events using near-real-time intensive aerosol optical properties in the north-western Mediterranean, Atmospheric Chemistry and Physics, 16, 12 567–12 586, 2016.

Ealo, M., Alastuey, A., Pérez, N., Ripoll, A., Querol, X., and Pandolfi, M.: Impact of aerosol particle sources on optical properties in urban, regional and remote areas in the north-western Mediterranean., Atmospheric Chemistry & Physics, 18, 2018.

Escudero, M., Castillo, S., Querol, X., Avila, A., Alarcón, M., Viana, M. M., Alastuey, A., Cuevas, E., and Rodríguez, S.: Wet and dry African dust episodes over eastern Spain, Journal of Geophysical Research: Atmospheres, 110, https://doi.org/10.1029/2004JD004731, https://agupubs.onlinelibrary.wiley.com/doi/abs/10.1029/2004JD004731, 2005.

Forello, A. C., Bernardoni, V., Calzolai, G., Lucarelli, F., Massabò, D., Nava, S., Pileci, R. E., Prati, P., Valentini, S., Valli, G., and Vecchi, R.: Exploiting multi-wavelength aerosol absorption coefficients in a multi-time source apportionment study to retrieve source-dependent absorption parameters, Atmospheric Chemistry and Physics Discussions, pp. 1–26, https://doi.org/10.5194/acp-2019-123, 2019.

Forello, A. C., Amato, F., Bernardoni, V., Calzolai, G., Canepari, S., Costabile, F., Di Liberto, L., Gualtieri, M., Lucarelli, F., Nava, S., Perrino, C., Petralia, E., Valentini, S., Valli, G., and Vecchi, R.: Gaining knowledge on source contribution to aerosol optical absorption properties and organics by receptor modelling, Atmospheric Environment, 243, 117 873, https://doi.org/10.1016/j.atmosenv.2020.117873, https://doi.org/10.1016/j.atmosenv.2020.117873, 2020.

Freedman, D. and Diaconis, P.: On the histogram as a density estimator:L2 theory, Zeitschrift für Wahrscheinlichkeitstheorie und Verwandte Gebiete, 57, 453–476, https://doi.org/10.1007/BF01025868, 1981.

GAW: GAW Report No. 226: Coupled Chemistry-Meteorology/Climate Modelling (CCMM): status and relevance for numerical weather prediction, atmospheric pollution and climate research, WMO, 1172, 2016.

Hansen, A., Rosen, H., and Novakov, T.: The aethaloemter- An instrument for the real-time measurement of optical absorption by particles, The Science of the Total Environment, 36, 191–196, 1984.

Houghton, J.T. Ding, Y. G. D. N. M. L. P. v. d. D. X. M. K. J. C.: Contribution of Working Group I to the Third Assessment Report of the Intergovernmental Panel on Climate Change, Cambridge University Press, p. 94, 2001.

Kalivitis, N., Gerasopoulos, E., Vrekoussis, M., Kouvarakis, G., Kubilay, N., Hatzianastassiou, N., Vardavas, I., and Mihalopoulos, N.: Dust transport over the eastern Mediterranean derived from Total Ozone Mapping Spectrometer, Aerosol Robotic Network, and surface measurements, Journal of Geophysical Research: Atmospheres, 112, 2007.

Kirchstetter, T. W., Novakov, T., and Hobbs, P. V.: Evidence that the spectral dependence of light absorption by aerosols is affected by organic carbon, Journal of Geophysical Research D: Atmospheres, 109, 1–12, https://doi.org/10.1029/2004JD004999, 2004a.

Kirchstetter, T. W., Novakov, T., and Hobbs, P. V.: Evidence that the spectral dependence of light absorption by aerosols is affected by organic carbon, Journal of Geophysical Research: Atmospheres, 109, 2004b.

Koçak, M., Mihalopoulos, N., and Kubilay, N.: Contributions of natural sources to high PM10 and PM2. 5 events in the eastern Mediterranean, Atmospheric Environment, 41, 3806–3818, 2007.

Lack, D. A., Lovejoy, E. R., Baynard, T., Pettersson, A., and Ravishankara, A. R.: Aerosol Absorption Measurement using Photoacoustic Spectroscopy: Sensitivity, Calibration, and Uncertainty Developments, Aerosol Science and Technology, 40, 697–708, https://doi.org/10.1080/02786820600803917, 2006.

Lack, D. A., Cappa, C. D., Covert, D. S., Baynard, T., Massoli, P., Sierau, B., Bates, T. S., Quinn, P. K., Lovejoy, E. R., and Ravishankara, A. R.: Bias in filter-based aerosol light absorption measurements due to organic aerosol loading: Evidence from ambient measurements, Aerosol Science and Technology, 42, 1033–1041, https://doi.org/10.1080/02786820802389277, 2008.

https://doi.org/10.5194/amt-2021-46
Preprint. Discussion started: 29 March 2021


Atmospheric Measurement Techniques Discussions

Lack, D. A., Moosmüller, H., McMeeking, G. R., Chakrabarty, R. K., and Baumgardner, D.: Characterizing elemental, equivalent black, and refractory black carbon aerosol particles: A review of techniques, their limitations and uncertainties, Analytical and Bioanalytical Chemistry, 406, 99–122, https://doi.org/10.1007/s00216-013-7402-3, 2014.

Laing, J. R., Jaffe, D. A., and Sedlacek, A. J.: Comparison of filter-based absorption measurements of biomass burning aerosol and background aerosol at the mt. Bachelor observatory, Aerosol and Air Quality Research, 20, 663–678, https://doi.org/10.4209/aaqr.2019.06.0298, 2020.

Laskin, A., Laskin, J., and Nizkorodov, S. A.: Chemistry of Atmospheric Brown Carbon, Chemical Reviews, 115, 4335–4382, https://doi.org/10.1021/cr5006167, 2015.

Lee, J. and Moosmüller, H.: Measurement of light absorbing aerosols with folded-jamin photothermal interferometry, Sensors (Switzerland), 20, 1–13, https://doi.org/10.3390/s20092615, 2020.

Lin, C. I., Baker, M., and Charlson, R. J.: Absorption Coefficient of Atmospheric Aerosol: a Method for Measurement., 1973.

Linke, C., Ibrahim, I., Schleicher, N., Hitzenberger, R., Andreae, M. O., Leisner, T., and Schnaiter, M.: A novel single-cavity three-wavelength photoacoustic spectrometer for atmospheric aerosol research, Atmospheric Measurement Techniques, 9, 5331–5346, https://doi.org/10.5194/amt-9-5331-2016, 2016.

Liousse, C., Cachier, H., and Jennings, S. G.: Optical and thermal measurements of black carbon aerosol content in different environments: Variation of the specific attenuation cross-section, sigma ($\sigma$), Atmospheric Environment Part A, General Topics, 27, 1203–1211, https://doi.org/10.1016/0960-1686(93)90246-U, 1993.

Liu, S., Aiken, A. C., Gorkowski, K., Dubey, M. K., Cappa, C. D., Williams, L. R., Herndon, S. C., Massoli, P., Fortner, E. C., Chhabra, P. S., Brooks, W. A., Onasch, T. B., Jayne, J. T., Worsnop, D. R., China, S., Sharma, N., Mazzoleni, C., Xu, L., Ng, N. L., Liu, D., Allan, J. D., Lee, J. D., Fleming, Z. L., Mohr, C., Zotter, P., Szidat, S., and Prévôt, A. S.: Enhanced light absorption by mixed source black and brown carbon particles in UK winter, Nature Communications, 6, https://doi.org/10.1038/ncomms9435, 2015.

Lyamani, H., Olmo, F., Alcántara, A., and Alados-Arboledas, L.: Atmospheric aerosols during the 2003 heat wave in southeastern Spain II: Microphysical columnar properties and radiative forcing, Atmospheric Environment, 40, 6465–6476, 2006.

Massabò, D., Bernardoni, V., Bove, M. C., Brunengo, A., Cuccia, E., Piazzalunga, A., Prati, P., Valli, G., and Vecchi, R.: A multi-wavelength optical set-up for the characterization of carbonaceous particulate matter, Journal of Aerosol Science, 60, 34–46, https://doi.org/10.1016/j.jaerosci.2013.02.006, 2013.

Mengis, N. and Matthews, H. D.: Non-CO2 forcing changes will likely decrease the remaining carbon budget for 1.5 °C, npj Climate and Atmospheric Science, 3, 1–7, https://doi.org/10.1038/s41612-020-0123-3, http://dx.doi.org/10.1038/s41612-020-0123-3, 2020.

Mona, L., Amodeo, A., Pandolfi, M., and Pappalardo, G.: Saharan dust intrusions in the Mediterranean area: Three years of Raman lidar measurements, Journal of Geophysical Research: Atmospheres, 111, 2006.

Moosmüller, H., Chakrabarty, R. K., and Arnott, W. P.: Aerosol light absorption and its measurement: A review, Journal of Quantitative Spectroscopy and Radiative Transfer, 110, 844–878, https://doi.org/10.1016/j.jqsrt.2009.02.035, 2009.

Müller, T.: Development of correction factors for Aethalometers AE31 and AE33, ACTRIS-2 WP3 Workshop, Athens, 10-12 November 2015, 2015.

Müller, T., Henzing, J., Leeuw, G. d., Wiedensohler, A., Alastuey, A., Angelov, H., Bizjak, M., Collaud Coen, M., Engström, J., Gruening, C., et al.: Characterization and intercomparison of aerosol absorption photometers: result of two intercomparison workshops, 2011a.

Müller, T., Laborde, M., Kassell, G., and Wiedensohler, A.: Design and performance of a three-wavelength LED-based total scatter and backscatter integrating nephelometer, Atmospheric Measurement Techniques, 4, 1291–1303, 2011b.

https://doi.org/10.5194/amt-2021-46
Preprint. Discussion started: 29 March 2021




Myhre, G., Shindell, D., Breéon, F.-M., Collins, W., Fuglestvedt, J., Huang, J., Koch, D., Lamarque, J.-F., Lee, D., Mendoza, B., Nakajima, T., Robock, A., Stephens, G., Takemura, T., and Zhang, H.: Anthropogenic and Natural Radiative Forcing, book section 8, p. 659–740, Cambridge University Press, Cambridge, United Kingdom and New York, NY, USA, https://doi.org/10.1017/CBO9781107415324.018, www.climatechange2013.org, 2013.

Ogren, J. A., Wendell, J., Andrews, E., and Sheridan, P. J.: Continuous light absorption photometer for long-Term studies, Atmospheric Measurement Techniques, 10, 4805–4818, https://doi.org/10.5194/amt-10-4805-2017, 2017.

Onasch, T. B., Massoli, P., Kebabian, P. L., Hills, F. B., Bacon, F. W., and Freedman, A.: Single scattering albedo monitor for airborne particulates, Aerosol Science and Technology, 49, 267–279, https://doi.org/10.1080/02786826.2015.1022248, 2015.

Pandolfi, M., Cusack, M., Alastuey, A., and Querol, X.: Variability of aerosol optical properties in the Western Mediterranean Basin, Atmospheric Chemistry and Physics, 11, 8189–8203, 2011.

Pandolfi, M., Querol, X., Alastuey, A., Jimenez, J., Jorba, O., Day, D., Ortega, A., Cubison, M., Comerón, A., Sicard, M., et al.: Effects of sources and meteorology on particulate matter in the Western Mediterranean Basin: An overview of the DAURE campaign, Journal of Geophysical Research: Atmospheres, 119, 4978–5010, 2014a.

Pandolfi, M., Ripoll, A., Querol, X., and Alastuey, A.: Climatology of aerosol optical properties and black carbon mass absorption cross section at a remote high-altitude site in the western Mediterranean Basin, Atmospheric Chemistry and Physics, 14, 6443–6460, 2014b.

Pandolfi, M., Tobias, A., Alastuey, A., Sunyer, J., Schwartz, J., Lorente, J., Pey, J., and Querol, X.: Effect of atmospheric mixing layer depth variations on urban air quality and daily mortality during Saharan dust outbreaks, Science of the Total Environment, 494, 283–289, 2014c.

Pandolfi, M., Alastuey, A., Pérez, N., Reche, C., Castro, I., Shatalov, V., and Querol, X.: Trends analysis of PM source contributions and chemical tracers in NE Spain during 2004–2014: a multi-exponential approach, Atmospheric Chemistry and Physics, 16, 11 787–11 805, 2016.

Pandolfi, M., Alados-Arboledas, L., Alastuey, A., Andrade, M., Angelov, C., Artiñano, B., Backman, J., Baltensperger, U., Bonasoni, P., Bukowiecki, N., Collaud Coen, M., Conil, S., Coz, E., Crenn, V., Dudoitis, V., Ealo, M., Eleftheriadis, K., Favez, O., Fetfatzis, P., Fiebig, M., Flentje, H., Ginot, P., Gysel, M., Henzing, B., Hoffer, A., Holubova Smejkalova, A., Kalapov, I., Kalivitis, N., Kouvarakis, G., Kristensson, A., Kulmala, M., Lihavainen, H., Lunder, C., Luoma, K., Lyamani, H., Marinoni, A., Mihalopoulos, N., Moerman, M., Nicolas, J., O'Dowd, C., Petäjä, T., Petit, J.-E., Pichon, J. M., Prokopciuk, N., Putaud, J.-P., Rodríguez, S., Sciare, J., Sellegri, K., Swietlicki, E., Titos, G., Tuch, T., Tunved, P., Ulevicius, V., Vaishya, A., Viana, M., Virkkula, A., Vratolis, S., Weingartner, E., Wiedensohler, A., and Laj, P.: A European aerosol phenomenology – 6: scattering properties of atmospheric aerosol particles from 28 ACTRIS sites, Atmospheric Chemistry and Physics, 18, 7877–7911, https://doi.org/10.5194/acp-18-7877-2018, https://www.atmos-chem-phys.net/18/7877/2018/, 2018.

Park, S. S., Hansen, A. D., and Cho, S. Y.: Measurement of real time black carbon for investigating spot loading effects of Aethalometer data, Atmospheric Environment, 44, 1449–1455, https://doi.org/10.1016/j.atmosenv.2010.01.025, http://dx.doi.org/10.1016/j.atmosenv.2010.01.025, 2010.

Pérez, N., Pey, J., Castillo, S., Viana, M., Alastuey, A., and Querol, X.: Interpretation of the variability of levels of regional background aerosols in the Western Mediterranean, Science of the total environment, 407, 527–540, 2008.

Petzold, A. and Schönlinner, M.: Multi-angle absorption photometry—a new method for the measurement of aerosol light absorption and atmospheric black carbon, Journal of Aerosol Science, 35, 421–441, 2004.

Petzold, A., Schloesser, H., Sheridan, P. J., Arnott, W. P., Ogren, J. A., and Virkkula, A.: Evaluation of multiangle absorption photometry for measuring aerosol light absorption, Aerosol Science and Technology, 39, 40–51, https://doi.org/10.1080/027868290901945, 2005.

https://doi.org/10.5194/amt-2021-46
Preprint. Discussion started: 29 March 2021


Atmospheric Measurement Techniques Discussions

Petzold, A., Ogren, J. A., Fiebig, M., Laj, P., Li, S. M., Baltensperger, U., Holzer-Popp, T., Kinne, S., Pappalardo, G., Sugimoto, N., Wehrli, C., Wiedensohler, A., and Zhang, X. Y.: Recommendations for reporting black carbon measurements, Atmospheric Chemistry and Physics, 13, 8365–8379, https://doi.org/10.5194/acp-13-8365-2013, 2013.

Pey, J., Pérez, N., Castillo, S., Viana, M., Moreno, T., Pandolfi, M., López-Sebastián, J., Alastuey, A., and Querol, X.: Geochemistry of regional background aerosols in the Western Mediterranean, Atmospheric Research, 94, 422–435, 2009.

Pey, J., Querol, X., Alastuey, A., Forastiere, F., and Stafoggia, M.: African dust outbreaks over the Mediterranean Basin during 2001–2011: PM 10 concentrations, phenomenology and trends, and its relation with synoptic and mesoscale meteorology, Atmospheric Chemistry and Physics, 13, 1395–1410, 2013.

Querol, X., Alastuey, A., Puicercus, J. A., Mantilla, E., Miro, J. V., Lopez-Soler, A., Plana, F., and Artiñano, B.: Seasonal evolution of suspended particles around a large coal-fired power station: particulate levels and sources, Atmospheric Environment, 32, 1963–1978, 1998.

Querol, X., Alastuey, A., Rodriguez, S., Plana, F., Ruiz, C. R., Cots, N., Massagué, G., and Puig, O.: PM10 and PM2. 5 source apportionment in the Barcelona Metropolitan area, Catalonia, Spain, Atmospheric Environment, 35, 6407–6419, 2001.

Querol, X., Alastuey, A., Viana, M. M., Rodriguez, S., Artíñano, B., Salvador, P., Do Santos, S. G., Fernandez Patier, R., Ruiz, C., De la Rosa, J., Sanchez de la Campa, A., Menendez, M., and Gil, J.: Speciation and origin of PM10 and PM2. 5 in Spain, Journal of Aerosol Science, 35, 1151–1172, 2004.

Querol, X., Alastuey, A., Pey, J., Cusack, M., Pérez, N., Mihalopoulos, N., Theodosi, C., Gerasopoulos, E., Kubilay, N., and Koçak, M.: Variability in regional background aerosols within the Mediterranean., Atmospheric Chemistry & Physics Discussions, 9, 2009a.

Querol, X., Pey, J., Pandolfi, M., Alastuey, A., Cusack, M., Pérez, N., Moreno, T., Viana, M., Mihalopoulos, N., Kallos, G., et al.: African dust contributions to mean ambient PM10 mass-levels across the Mediterranean Basin, Atmospheric Environment, 43, 4266–4277, 2009b.

Querol, X., Perez, N., Reche, C., Ealo, M., Ripoll, A., Tur, J., Pandolfi, M., Pey, J., Salvador, P., Moreno, T., et al.: African dust and air quality over Spain: Is it only dust that matters?, Science of the total environment, 686, 737–752, 2019.

Ramanathan, V. and Carmichael, G.: Global and regional climate changes due to black carbon, Nature Geoscience, 1, 221–227, https://doi.org/10.1038/ngeo156, 2008.

Ramanathan, V., Crutzen, P. J., Kiehl, J. T., and Rosenfeld, D.: Aerosols , Climate , and the Hydrological Cycle, 294, 2119–2124, 2020.

Reche, C., Querol, X., Alastuey, A., Viana, M., Pey, J., Moreno, T., Rodríguez, S., González, Y., Fernández-Camacho, R., Rosa, J., et al.: New considerations for PM, Black Carbon and particle number concentration for air quality monitoring across different European cities, Atmospheric Chemistry and Physics, 11, 6207–6227, 2011.

Rigler, M., Drinovec, L., Lavri, G., Vlachou, A., Prevot, A. S., Luc Jaffrezo, J., Stavroulas, I., Sciare, J., Burger, J., Kranjc, I., Turšič, J., D. A. Hansen, A., and Mocnik, G.: The new instrument using a TC-BC (total carbon-black carbon) method for the online measurement of carbonaceous aerosols, Atmospheric Measurement Techniques, 13, 4333–4351, https://doi.org/10.5194/amt-13-4333-2020, 2020.

Ripoll, A., Pey, J., Minguillón, M. C., Pérez, N., Pandolfi, M., Querol, X., and Alastuey, A.: Three years of aerosol mass, black carbon and particle number concentrations at Montsec (southern Pyrenees, 1570 m asl), Atmospheric Chemistry and Physics, 14, 4279–4295, 2014.

Ripoll, A., Minguillón, M. C., Pey, J., Jimenez, J. L., Day, D. A., Sosedova, Y., Canonaco, F., Prévôt, A. S., Querol, X., and Alastuey, A.: Long-term real-time chemical characterization of submicron aerosols at Montsec (southern Pyrenees, 1570 m a.s.l.), Atmospheric Chemistry and Physics, 15, 2935–2951, https://doi.org/10.5194/acp-15-2935-2015, 2015.

https://doi.org/10.5194/amt-2021-46
Preprint. Discussion started: 29 March 2021


Atmospheric Measurement Techniques Discussions

Rivas, I., Beddows, D. C., Amato, F., Green, D. C., Järvi, L., Hueglin, C., Reche, C., Timonen, H., Fuller, G. W., Niemi, J. V., et al.: Source apportionment of particle number size distribution in urban background and traffic stations in four European cities, Environment International, 135, 105 345, 2020.

Rodrıguez, S., Querol, X., Alastuey, A., Kallos, G., and Kakaliagou, O.: Saharan dust contributions to PM10 and TSP levels in Southern and Eastern Spain, Atmospheric Environment, 35, 2433–2447, 2001.

Rodríguez, S., Querol, X., Alastuey, A., and Plana, F.: Sources and processes affecting levels and composition of atmospheric aerosol in the western Mediterranean, Journal of Geophysical Research: Atmospheres, 107, AAC–12, 2002.

Samset, B. H., Sand, M., Smith, C. J., Bauer, S. E., Forster, P. M., Fuglestvedt, J. S., Osprey, S., and Schleussner, C. F.: Climate Impacts From a Removal of Anthropogenic Aerosol Emissions, Geophysical Research Letters, 45, 1020–1029, https://doi.org/10.1002/2017GL076079, 2018.

Sandradewi, J., Prévôt, A. S., Szidat, S., Perron, N., Alfarra, M. R., Lanz, V. A., Weingartner, E., and Baltensperger, U. R.: Using aerosol light absorption measurements for the quantitative determination of wood burning and traffic emission contribution to particulate matter, Environmental Science and Technology, 42, 3316–3323, https://doi.org/10.1021/es702253m, 2008.

Schauer, G., Kasper-Giebl, A., and Močnik, G.: Increased PM concentrations during a combined wildfire and saharan dust event observed at high-altitude Sonnblick observatory, Austria, Aerosol and Air Quality Research, 16, 542–554, https://doi.org/10.4209/aaqr.2015.05.0337, 2016.

Schmid, O., Artaxo, P., Arnott, W. P., Chand, D., Gatti, L. V., Frank, G. P., Hoffer, A., Schnaiter, M., and Andreae, M. O.: Spectral light absorption by ambient aerosols influenced by biomass burning in the Amazon Basin. I: Comparison and field calibration of absorption measurement techniques, Atmospheric Chemistry and Physics, 6, 3443–3462, https://doi.org/10.5194/acp-6-3443-2006, 2006.

Segura, S., Estellés, V., Titos, G., Lyamani, H., Utrillas, M. P., Zotter, P., Prévôt, A. S., Močnik, G., Alados-Arboledas, L., and Martínez-Lozano, J. A.: Determination and analysis of in situ spectral aerosol optical properties by a multi-instrumental approach, Atmospheric Measurement Techniques, 7, 2373–2387, https://doi.org/10.5194/amt-7-2373-2014, 2014.

Sheridan, P. J., Patrick Arnott, W., Ogren, J. A., Andrews, E., Atkinson, D. B., Covert, D. S., Moosmüller, H., Petzold, A., Schmid, B., Strawa, A. W., Varma, R., and Virkkula, A.: The reno aerosol optics study: An evaluation of aerosol absorption measurement methods, Aerosol Science and Technology, 39, 1–16, https://doi.org/10.1080/027868290901891, 2005.

Singh, S., Fiddler, M. N., Smith, D., and Bililign, S.: Error analysis and uncertainty in the determination of aerosol optical properties using cavity ring-down spectroscopy, integrating nephelometry, and the extinction-minus-scattering method, Aerosol Science and Technology, 48, 1345–1359, https://doi.org/10.1080/02786826.2014.984062, 2014.

Springston, S. R. and Sedlacek, A. J.: Noise characteristics of an instrumental particle absorbance technique, Aerosol Science and Technology, 41, 1110–1116, https://doi.org/10.1080/02786820701777457, 2007.

Stephens, M., Turner, N., and Sandberg, J.: Particle identification by laser-induced incandescence in a solid-state laser cavity, Applied Optics, 42, 3726, https://doi.org/10.1364/ao.42.003726, 2003.

Terhune, R. W. and Anderson, J. E.: Spectrophone measurements of the absorption of visible light by aerosols in the atmosphere, Optics Letters, 1, 70, https://doi.org/10.1364/ol.1.000070, 1977.

Valentini, S., Barnaba, F., Bernardoni, V., Calzolai, G., Costabile, F., Di Liberto, L., Forello, A. C., Gobbi, G. P., Gualtieri, M., Lucarelli, F., Nava, S., Petralia, E., Valli, G., Wiedensohler, A., and Vecchi, R.: Classifying aerosol particles through the combination of optical and physical-chemical properties: Results from a wintertime campaign in Rome (Italy), Atmospheric Research, 235, 104 799, https://doi.org/10.1016/j.atmosres.2019.104799, https://doi.org/10.1016/j.atmosres.2019.104799, 2020a.



Valentini, S., Bernardoni, V., Bolzacchini, E., Ciniglia, D., Pandolfi, M., Ferrero, L., Forello, A. C., Massabó, D., Pandolfi, M., Prati, P., Soldan, F., Valli, G., Yus-díez, J., and Vecchi, R.: Applicability of benchtop multi-wavelength polar photometers to off-line measurements of the Multi-Angle Absorption Photometer, pp. 1–13, https://doi.org/10.1016/j.jaerosci.2020.105701, 2020b.

Vecchi, R., Bernardoni, V., Paganelli, C., and Valli, G.: A filter-based light-absorption measurement with polar photometer: Effects of sampling artefacts from organic carbon, Journal of Aerosol Science, 70, 15–25, 2014.

Virkkula, A., Mäkelä, T., Hillamo, R., Yli-Tuomi, T., Hirsikko, A., Hämeri, K., and Koponen, I. K.: A simple procedure for correcting loading effects of aethalometer data, Journal of the Air and Waste Management Association, 57, 1214–1222, https://doi.org/10.3155/1047-3289.57.10.1214, 2007.

Virkkula, A., Chi, X., Ding, A., Shen, Y., Nie, W., Qi, X., Zheng, L., Huang, X., Xie, Y., Wang, J., Petäjä, T., and Kulmala, M.: On the interpretation of the loading correction of the aethalometer, Atmospheric Measurement Techniques, 8, 4415–4427, https://doi.org/10.5194/amt-8-4415-2015, 2015.

Visser, B., Röhrbein, J., Steigmeier, P., Drinovec, L., Močnik, G., and Weingartner, E.: A single-beam photothermal interferometer for in-situ measurements of aerosol light absorption, Atmospheric Measurement Techniques Discussions, 2, 1–24, https://doi.org/10.5194/amt-2020-242, 2020.

Wang, Y., Le, T., Chen, G., Yung, Y. L., Su, H., Seinfeld, J. H., and Jiang, J. H.: Reduced European aerosol emissions suppress winter extremes over northern Eurasia, Nature Climate Change, 10, 225–230, https://doi.org/10.1038/s41558-020-0693-4, http://dx.doi.org/10.1038/s41558-020-0693-4, 2020.

Weingartner, E., Saathoff, H., Schnaiter, M., Streit, N., Bitnar, B., and Baltensperger, U.: Absorption of light by soot particles: Determination of the absorption coefficient by means of aethalometers, Journal of Aerosol Science, 34, 1445–1463, https://doi.org/10.1016/S0021-8502(03)00359-8, 2003.

WMO: WMO/GAW Aerosol Measurement Procedures, Guidelines and Recommendations, WMO- No. 1177; GAW Report- No. 227, https://library.wmo.int/doc{_}num.php?explnum{_}id=3073, 2016.

Yus-Díez, J., Ealo, M., Pandolfi, M., Perez, N., Titos, G., Močnik, G., Querol, X., and Alastuey, A.: Aircraft vertical profiles during summertime regional and Saharan dust scenarios over the north-western Mediterranean Basin: aerosol optical and physical properties, Atmospheric Chemistry and Physics Discussions, pp. 1–35, 2020.

Zanatta, M., Gysel, M., Bukowiecki, N., Müller, T., Weingartner, E., Areskoug, H., Fiebig, M., Yttri, K. E., Mihalopoulos, N., Kouvarakis, G., et al.: A European aerosol phenomenology-5: Climatology of black carbon optical properties at 9 regional background sites across Europe, Atmospheric environment, 145, 346–364, 2016.

Zhang, Y., Favez, O., Canonaco, F., Liu, D., Močnik, G., Amodeo, T., Sciare, J., Prévôt, A. S. H., Gros, V., and Albinet, A.: Evidence of major secondary organic aerosol contribution to lensing effect black carbon absorption enhancement, npj Climate and Atmospheric Science, 1, https://doi.org/10.1038/s41612-018-0056-2, 2018.

Zotter, P., Herich, H., Gysel, M., El-Haddad, I., Zhang, Y., Mocnik, G., Hüglin, C., Baltensperger, U., Szidat, S., and Prévôt, A. S.: Evaluation of the absorption Ångström exponents for traffic and wood burning in the Aethalometer-based source apportionment using radiocarbon measurements of ambient aerosol, Atmospheric Chemistry and Physics, 17, 4229–4249, https://doi.org/10.5194/acp-17-4229-2017, 2017.